

1 **GENOME-WIDE ASSOCIATIONS OF AORTIC DISTENSIBILITY SUGGEST CAUSAL**
2 **RELATIONSHIPS WITH AORTIC ANEURYSMS AND BRAIN WHITE MATTER**
3 **HYPERINTENSITIES**

4
5 Catherine M Francis^{1,2*}, Matthias E Futschik^{3,4*}, Jian Huang^{3*}, Wenjia Bai^{5,6}, Muralidharan
6 Sargurupremraj^{7,8}, Enrico Petretto^{9,10,11}, Amanda SR Ho¹¹, Philippe Amouyel^{12,13,14,15}, Stefan T
7 Engelter^{16,17}, James S Ware^{1,4,2}, Stephanie Debette^{8,18}, Paul Elliott^{3,19,20,21,22,23}, Abbas Dehghan^{3,19§},
8 Paul M Matthews^{5,19,22§}
9

10 ¹National Heart and Lung Institute, Imperial College London, Programme in Cardiovascular Genetics and
11 Genomics; ²Royal Brompton and Harefield Hospitals, London UK; ³Department of Epidemiology and
12 Biostatistics, School of Public Health, Imperial College London, London, UK; ⁴MRC London Institute of Medical
13 Sciences (LMS), Imperial College London, London W12 0NN, UK; ⁵Department of Brain Sciences, Imperial
14 College London, London, UK; ⁶Department of Computing, Imperial College London, London, UK; ⁷Glenn Biggs
15 Institute for Alzheimer's & Neurodegenerative Diseases, University of Texas Health Sciences Center, San
16 Antonio, TX 78229, USA; ⁸University of Bordeaux, Inserm, Bordeaux Population Health Research Center,
17 team VINTAGE, UMR 1219, 33000 Bordeaux, France; ⁹ Programme in Cardiovascular & Metabolic Disorders
18 and Centre for Computational Biology, Duke-NUS Medical School, Singapore 169857, Republic of Singapore;
19 ¹⁰ Institute of Big Data and Artificial Intelligence, China Pharmaceutical University (CPU), 211198 Nanjing,
20 China; ¹¹Computational Biology Programme, Faculty of Science, National University of Singapore
21 ¹²LabEx DISTALZ-U1167, RID-AGE-Risk Factors and Molecular Determinants of Aging-Related Diseases,
22 University of Lille, Lille, France; ¹³Inserm U1167, Lille, France; ¹⁴Centre Hospitalier Universitaire Lille, Lille,
23 France; ¹⁵Institut Pasteur de Lille, Lille, France; ¹⁶Department of Neurology and Stroke Center, University
24 Hospital and University of Basel, Petersgraben 4, CH – 4031 Basel, Switzerland; ¹⁷Department of Clinical
25 Neurology and Neurorehabilitation, University Department of Geriatric Medicine FELIX PLATTER, University
26 of Basel; ¹⁸Department of Neurology, Institute for Neurodegenerative Diseases, Bordeaux University Hospital
27 – CHU Bordeaux, 33000 Bordeaux, France; ¹⁹UK Dementia Research Institute at Imperial College London,
28 London, UK; ²⁰Health Data Research (HDR) UK London at Imperial College London, London, UK; ²¹British
29 Heart Foundation Centre of Research Excellence at Imperial College London, London, UK; ²²National Institute
30 for Health Research Imperial Biomedical Research Centre, Imperial College London, London, UK; ²³MRC
31 Centre for Environment and Health, School of Public Health, Imperial College London, London, UK
32

33 *joint first authors

34 §corresponding author

35
36 Abbas Dehghan, MD, PhD
37 Reader in Cardiometabolic Disease Epidemiology
38 Department of and Biostatistics
39 School of Public Health, Faculty of Medicine
40 Imperial College London
41 St Mary's Campus
42 Norfolk Place, LONDON, W2 1PG
43 Tel: +44 (0)20 7594 3347
44 a.dehghan@imperial.ac.uk

45 Paul M. Matthews, MD, DPhil
46 Head of Department
47 E515, Department of Brain Sciences
48 Imperial College London
49 Hammersmith Hospital
50 DuCane Road, London WC12 0NN
51 Tel: 0044 207 594 2612
52 p.matthews@imperial.ac.uk
53

54 **NOTE: This preprint reports new research that has not been certified by peer review and should not be used to guide clinical practice.**

55
56
57
58
59
60
61
62
63
64
65
66
67
68
69
70
71
72
73

ABSTRACT

Aortic dimensions and distensibility are key risk factors for aortic aneurysms and dissections, as well as for other cardiovascular and cerebrovascular diseases. We tested genome-wide associations of ascending and descending aortic distensibility and area derived from cardiac magnetic resonance imaging (MRI) data of up to 32,590 Caucasian individuals in UK Biobank. We identified 102 loci (including 31 novel associations) tagging genes related to cardiovascular development, extracellular matrix production, smooth muscle cell contraction and heritable aortic diseases. Functional analyses highlighted four signalling pathways associated with aortic distensibility (TGF- β , IGF, VEGF and PDGF). We identified distinct sex-specific associations with aortic traits. We developed co-expression networks associated with aortic traits and applied phenome-wide Mendelian randomization (MR-PheWAS), generating evidence for a causal role for aortic distensibility in development of aortic aneurysms. Multivariable MR suggested a causal relationship between aortic distensibility and cerebral white matter hyperintensities, mechanistically linking aortic traits and brain small vessel disease.

74 INTRODUCTION

75 The aorta acts as both conduit and buffer¹, conveying oxygenated blood from the heart to the
76 systemic circulation, and dampening the pulse pressure to which peripheral circulations are
77 subjected. Diseases affecting the aorta are common and their complications are associated with a
78 high mortality even in young people. Quantitative aortic traits (aortic dimensions and functional
79 measures) can predict progression of these aortopathies. For example, the elastic function of the
80 thoracic aorta and aortic dimensions are key determinants of rates of growth of thoracic aortic
81 aneurysms²⁻⁴. At a population level, aortic traits are also clinically important predictors of risks of
82 cardiovascular and cerebrovascular diseases⁵⁻¹⁰.

83

84 The decline in elastic function with age may be measured as a decrease in distensibility, a factor
85 independently predictive of cerebral microvascular disease, the development of age-related
86 dementia and neurodegenerative changes of Alzheimer's Disease (AD)¹¹⁻¹³. Recent data also have
87 provided evidence for an association of aortic distensibility with cognitive performance in the general
88 population¹⁴. White matter hyperintensities (WMH) represent the most common brain imaging
89 feature of small vessel disease and predict mortality and morbidity with aging (including risks of
90 stroke (ischemic and hemorrhagic), dementia, and functional impairment¹⁵⁻¹⁸). Aortic stiffness is a
91 stronger predictor of WMH volume than blood pressure or hypertension alone^{19, 20} and has effects
92 additive to those of hypertension in predicting WMH¹⁹⁻²¹. The genomic bases of these relationships
93 have not been well explored to date.

94

95 With age, aortic stiffening arises from changes in composition of the aortic wall, including
96 degradation of the elastic fibres and decreased cellularity, along with a relative increase in the
97 collagen content of the aorta (although the absolute amount decreases)^{22, 23}. In addition, extracellular
98 matrix proteins themselves undergo conformational and biochemical changes which alter their
99 passive mechanical properties. These remodelling processes are driven by TGF- β signalling
100 pathways and accelerated by oxidative stress and inflammation²⁴ acting on the cells in the aortic
101 wall. These cellular and molecular drivers of worsening aortic elastic function are reflected in
102 macroscopic changes with age.

103

104 Here, we used convolutional neural networks for automated aortic segmentation²⁵ to measure
105 ascending and descending aortic areas and distensibilities on cardiac magnetic resonance (MRI)
106 images from UK Biobank, which is currently the largest cardiac imaging epidemiological study²⁶. We
107 have described our approach to derivation of imaging derived quantitative aortic traits and the
108 distribution of these traits in a smaller group from the same population in an earlier report^{25, 27}. We
109 derived six aortic traits (ascending aortic distensibility (AAdis), descending aortic distensibility
110 (DAdis), maximum ascending aortic area (AAMax), minimum ascending aortic area (AAmin),

111 maximum descending aortic area (DAm_{ax}) and minimum descending aortic area (DA_{min}) in up to
112 32,590 (depending on the specific trait) UK Biobank participants, who were free from known aortic
113 disease. We then performed a genome-wide association study (GWAS) of the six CMR-derived
114 aortic traits and carried out functional analyses and a series of Mendelian Randomization studies to
115 investigate possible causal associations of the aortic measures with aortic aneurysms and brain
116 small vessel disease. We also explored the bidirectional relationship of aortic traits with indices of
117 blood pressure.

118

119 **RESULTS**

120

121 Study cohort exclusions are presented in Supplementary Figure S1. The distributions of the aortic
122 traits are shown in Supplementary Figure S2.

123

124 ***SNP-based heritability***

125 We estimated the proportion of the variability in aortic traits that could be attributed to common
126 genetic variation from an analysis of SNP-based heritability (h^2_{SNP}) using linkage disequilibrium
127 score regression (LDSC). h^2_{SNP} estimates ranged from 0.10 (for DA_{dis} single trait) to 0.41 (for
128 AA_{max}). We also tested for heritability of distensibility traits using multi-trait analysis (MTAG, h^2_{SNP}
129 =0.21 for DA_{dis} and h^2_{SNP} =0.24 for AA_{dis}).

130

131 ***Phenotypic and genotypic correlations between traits***

132 We found strong phenotypic and genotypic correlations between maximum and minimum aortic
133 areas (phenotypic $r=0.99$, $p<2.2\times 10^{-16}$; genotypic $r_g=0.99$, $p<1\times 10^{-50}$ for the ascending aorta;
134 phenotypic $r=0.98$, $p<2.2\times 10^{-16}$; genotypic $r_g=0.99$, $p<1\times 10^{-50}$ for the descending aorta). There were
135 lower correlations between ascending and descending aortic traits (phenotypic $r=0.60$, $p<2.2\times 10^{-16}$
136 and genotypic $r_g=0.45$, $p<1.7\times 10^{-25}$ for the minimum aortic areas and phenotypic $r=0.74$, $p<2.2\times 10^{-16}$
137 and genotypic $r_g=0.45$, $p<9.25\times 10^{-7}$ for distensibilities) consistent with known biological and
138 functional differences along the course of the aorta¹. Correlations are presented in Supplementary
139 Figures S3 and S4.

140

141 ***Single and multi-trait aortic GWAS***

142 Our stage 1 GWAS (N=32,590 for areas and N=29,895 for distensibility) identified a total of 95
143 significant loci (using a genome-wide significance threshold of $p<5\times 10^{-8}$) across the six traits, 94 of
144 which are autosomal with one localised to the X chromosome. Genomic inflation was within
145 acceptable limits for all traits ($\lambda=1.147$ for the area traits; $\lambda=1.047$ for the distensibility traits). We
146 took advantage of the correlation between the aortic traits to enhance power for discovery of loci by
147 performing multi-trait analysis (MTAG)²⁸ as a second stage of our GWAS. Use of MTAG combining

148 all six phenotypes increased the number of significant loci for the distensibility traits from 10 to 26 for
149 the ascending aorta and from 7 to 13 for the descending aorta (Table 1), and the total number of
150 significant loci across all aortic traits to 102. Figure 1A shows the Manhattan and QQ plots from
151 GWAS of ascending and descending aortic minimum areas, which overlap almost completely with
152 the findings for the corresponding maximum areas. Figure 1B shows the results of the MTAG
153 analysis of ascending and descending aortic distensibilities. GWAS summary statistics from
154 9,753,033 variants with a minor allele frequency (MAF) ≥ 0.01 for the stage 1 and stage 2 (MTAG)
155 analyses are shown in Supplementary Figures S5-S8.

156
157 Individual loci were annotated with *cis*-expression quantitative trait loci (eQTL) and splice
158 quantitative trait loci (sQTL) data from GTEx v8²⁹. Twenty-four of the 38 loci associated with
159 distensibilities had lead SNPs which were significant eQTLs or sQTLs for nearby genes in arterial
160 tissue.

161

162

163

Locus	Lead SNP rsID	Chr	BP	Annotation	Closest gene	Effect allele	MAF	No. of lead SNPs	Beta	P	Trait association reaching genome-wide significance
1*	rs835341	1	53064012	intergenic	GPX7	A	0.41	1	0.027	7.78E-09	AAdis
2	rs824510	2	19725556	intergenic	AC010096.2	G	0.32	1	0.037	3.73E-14	AAdis
3	rs9306895	2	20878153	ncRNA_exonic	AC012065.7: RP11-130L8.1	T	0.37	1	0.038	4.87E-17	DAdis
4	<i>rs6724315</i>	<i>2</i>	<i>46363699</i>	<i>intronic</i>	<i>PRKCE</i>	<i>T</i>	<i>0.15</i>	<i>1</i>	<i>-0.053</i>	<i>3.00E-08#</i>	<i>DAdis</i>
5	rs35303331	2	164921770	ncRNA_intronic	AC092684.1	A	0.22	1	0.031	2.04E-08	AAdis
6	<i>rs541051407</i>	<i>3</i>	<i>41871295</i>	<i>intronic</i>	<i>ULK4</i>	<i>G</i>	<i>0.15</i>	<i>1</i>	<i>-0.058</i>	<i>2.20E-08#</i>	<i>AAdis</i>
7*	rs7638565	3	64723072	ncRNA_intronic	ADAMTS9-AS2	A	0.43	1	0.026	4.53E-08	AAdis
8	rs55914222	3	128202943	intronic	GATA2	G	0.02	1	-0.086	8.48E-10	AAdis
9	rs79957887	3	187006335	intronic	MASP1	C	0.06	1	0.054	3.14E-11	DAdis
10	rs17020769	4	146800922	intronic	ZNF827	C	0.44	1	0.025	4.00E-08	AAdis
11*	rs13158444	5	51201361	intergenic	RNA5SP182	T	0.38	1	-0.027	9.61E-09	AAdis
12	rs79051849	5	81848970	intergenic	CTD-2015A6.1	A	0.20	1	-0.039	5.29E-11	AAdis
13	rs201281936	5	95606717	ncRNA_intronic	CTD-2337A12.1: RP11-254I22.2	A	0.34	2	-0.053	4.79E-28	AAdis
14	rs337101	5	122550646	intergenic	PRDM6	T	0.30	2	0.034	2.93E-11	AAdis
15	rs2490445	6	12544672	intergenic	RPL15P3	T	0.29	1	0.028	2.29E-08	AAdis
16*	rs1406667	6	122178493	downstream	HMGB3P18	A	0.11	1	0.043	3.53E-09	DAdis
17	rs56072713	7	73427710	intergenic	ELN	G	0.47	1	0.034	1.83E-15	DAdis
17	rs7795735	7	73429482	intergenic	ELN	T	0.46	4	0.077	4.78E-62	AAdis
18	rs9721183	8	75781818	intergenic	RP11-758M4.4	C	0.40	1	-0.033	1.39E-11	AAdis
19*	rs7832313	8	92198211	intronic	LRRC69	G	0.33	1	0.026	1.48E-08	DAdis
20	rs11992999	8	122639443	intronic	HAS2	T	0.25	1	-0.038	4.42E-14	AAdis
21	rs34557926	8	124607159	intergenic	RN7SKP155	C	0.37	1	0.039	7.75E-16	AAdis
21	rs7006122	8	124608614	intergenic	RN7SKP155	T	0.38	2	0.030	1.54E-11	DAdis
22	rs9702161	10	30077914	intergenic	SVIL	T	0.29	1	-0.029	1.52E-08	AAdis
22	rs7096778	10	30165983	intergenic	RP11-224P11.1; SVIL	T	0.41	2	-0.030	3.75E-12	DAdis
23	<i>rs10857614</i>	<i>10</i>	<i>49829983</i>	<i>intronic</i>	<i>ARHGAP22</i>	<i>T</i>	<i>0.48</i>	<i>1</i>	<i>0.034</i>	<i>4.10E-08#</i>	<i>AAdis</i>
24	rs10761716	10	64882300	intergenic	RP11-144G16.1	C	0.45	1	-0.026	4.34E-08	AAdis
25	rs78629306	10	95897188	intronic	PLCE1	G	0.20	2	0.039	2.76E-10	AAdis
25	rs61886305	10	95902053	intronic	PLCE1	C	0.20	6	0.051	2.49E-19	DAdis
26	rs875106	11	70005641	intronic	ANO1	G	0.49	2	-0.027	8.77E-09	AAdis
27	rs11046213	12	22008367	ncRNA_intronic	ABCC9:RP11- 729I10.2	G	0.38	1	-0.032	1.18E-11	AAdis
28*	rs61927702	12	33631695	intergenic	RP11-56H16.1	A	0.44	1	-0.026	2.87E-09	DAdis
29	rs12863716	13	22862729	intergenic	MTND3P1	C	0.20	1	-0.042	1.23E-13	AAdis
30*	rs8014161	14	92393198	intronic	FBLN5	T	0.35	1	-0.032	1.91E-12	DAdis
31	rs1441358	15	71612514	intronic	THSD4	T	0.36	1	-0.032	6.42E-11	AAdis
32	rs77870048	16	69965021	intronic	WWP2	C	0.04	1	-0.066	1.59E-10	AAdis
33*	rs3851734	16	75371920	intronic	CFDP1	T	0.44	1	-0.029	2.98E-11	DAdis
34	<i>rs2228685</i>	<i>16</i>	<i>83065965</i>	<i>intronic</i>	<i>CDH13</i>	<i>T</i>	<i>0.47</i>	<i>1</i>	<i>0.037</i>	<i>2.80E-09#</i>	<i>AAdis</i>
35	rs28375406	16	88996841	intronic	CBFA2T3	A	0.35	1	-0.026	3.88E-08	AAdis
36	rs57130712	17	2089035	intronic	SMG6	A	0.31	3	0.042	3.46E-17	AAdis
36	rs1532292	17	2097483	intronic	SMG6	T	0.40	1	0.027	5.57E-10	DAdis
37*	rs112009052	19	41099501	intronic	LTBP4	T	0.01	1	-0.105	2.46E-08	DAdis
38*	rs28451064	21	35593827	ncRNA_intronic	AP000320.7: AP000318.2	G	0.13	1	-0.039	1.39E-08	AAdis

164

165

166

167

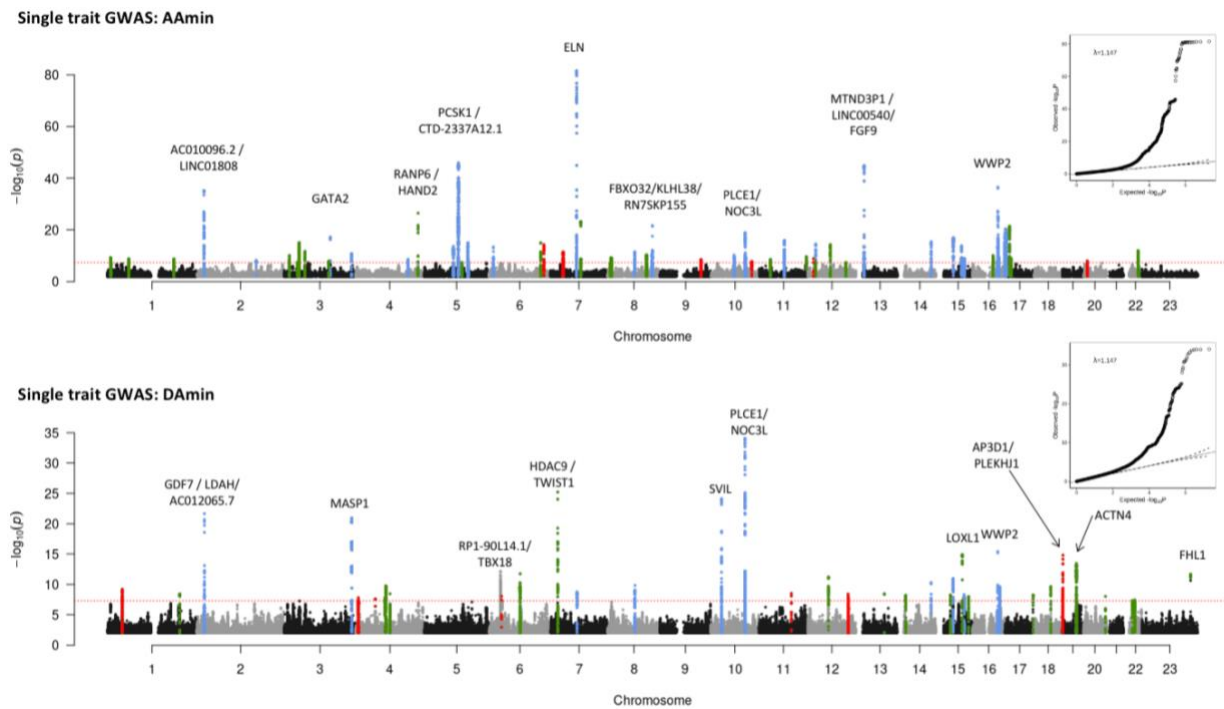
168

169

170

TABLE 1: Significant associations with distensibility in single and multi-trait genome-wide analyses. Summary statistics are shown for lead SNPs which were genome-wide significant ($p < 5 \times 10^{-8}$) in MTAG analysis (loci in black) apart from the four loci (in green and blue) which were significant in single trait analysis only. Where loci overlapped, different lead SNPs are listed separately under the same locus number. Green = genome-wide significant in only the single trait analysis, not the multi-trait analysis, but also significantly associated with aortic area traits. MAF=

171 Minor Allele Frequency; Chr=chromosome, BP= position (GRCh37). Blue = genome-wide
 172 significant in only the single trait analysis of distensibility and in no other aortic traits. *=novel locus
 173 not identified in previous GWAS of ascending or descending aortic traits.
 174
 175
 176



177

178 **FIGURE 1A: Manhattan plots of summary statistics from single-trait GWAS of aortic areas.**
 179 Red dashed line shows the genome-wide significance threshold of $P = 5 \times 10^{-8}$. Genomic inflation (λ)
 180 = 1.147 (AMin and DMin). Annotations of selected loci show the nearest gene and additional
 181 manual annotation of likely candidate gene(s) at the locus where appropriate. Blue: locus is
 182 genome-wide significant in multiple aortic traits, green: locus is genome wide significant only in the
 183 corresponding trait and with nominal significance ($p < 0.01$) in other traits, red: genome-wide
 184 significant only in the corresponding trait without even nominal significance in other traits. QQ plots
 185 are shown as inserts in corresponding panels.

186

187

188

189

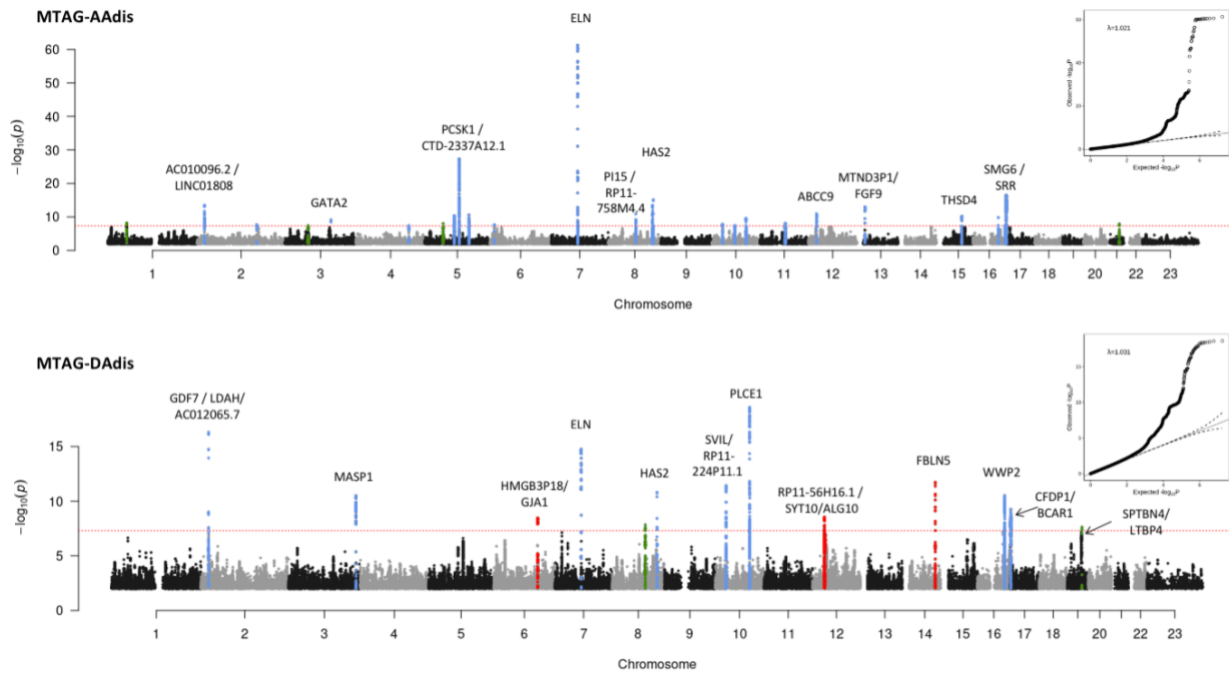
190

191

192

193

194



195

196 **FIGURE 1B: Manhattan plots of summary statistics from multi-trait GWAS (MTAG) of aortic**
197 **distensibility.** All six traits were used for the MTAG analysis. Twenty-six association signals were
198 identified in multi-trait analysis of AAdis and thirteen in multi-trait analysis of DADis. Genomic
199 inflation (λ) = 1.021 (AAdis) and 1.031 (DADis). Red dashed line shows the genome-wide
200 significance threshold of $P = 5 \times 10^{-8}$. Blue: locus is genome-wide significant in multiple aortic traits,
201 green: locus is genome wide significant only in the corresponding trait and with nominal significance
202 ($p < 0.01$) in other traits, red: genome-wide significant only in the corresponding trait without even
203 nominal significance in other traits. QQ plots are shown as inserts in corresponding panels.

204

205

206

207

208

209

210 The most significant associations with ascending aortic distensibility were: rs7795735, 12.6
211 kilobases upstream of *ELN*, a gene encoding elastin; rs201281936, which is in a lncRNA (*CTD-*
212 *2337A12.1*) 119 kilobases 3' of *PCSK1* (Proprotein Convertase Subtilisin/Kexin Type 1);
213 rs57130712, which is in a locus spanning *SMG6* (*SMG6* Nonsense Mediated mRNA Decay Factor)
214 and *SRR* (Serine Racemase), and which is the most significant eQTL for *SRR* in arterial tissue
215 ($p=2 \times 10^{-20}$, normalised effect size (NES)= -0.39)²⁹; and rs34557926, an intronic variant in *HAS2*
216 (Hyaluronan Synthase 2).

217
218 The strongest associations with descending aortic distensibility were different. The most significant
219 association was with rs61886305, an intronic variant in *PLCE1* (Phospholipase C Epsilon 1). This
220 lead SNP is a strong eQTL for *PLCE1* in arterial tissue ($p=1.1 \times 10^{-8}$, NES= -0.20)²⁹. The next
221 strongest association was with rs9306895, an intronic variant in *GDF7* (Growth Differentiation Factor
222 7), which is a strong eQTL for both *GDF7* and *LDAH* (Lipid Droplet Associated Hydrolase) in aorta²⁹
223 (*GDF7*: $p=3.6 \times 10^{-9}$, NES= 0.20; *LDAH*: $p=7.1 \times 10^{-28}$, NES= 0.53). A locus spanning *ELN* was
224 associated with DAdis, with the lead SNP less than 1.8kb away from the lead SNP for AAdis at this
225 locus, and in strong LD with it ($R^2=0.96$; $D'=1$). A locus in *FBLN5* (lead SNP rs8014161) was
226 associated with descending, but not ascending distensibility.

227
228 There were four loci associated at genome-wide significance with aortic distensibilities which lost
229 genome-wide significance in the MTAG analysis (three associated with AAdis and one with DAdis;
230 see Table 1 for details). Two of these were not significantly associated with any other aortic traits:
231 rs6724315 in *PRKCE* and rs10857614 in *ARHGAP22*. The latter is a strong eQTL for *ARHGAP22* in
232 aorta ($p=2.6 \times 10^{-46}$, NES= 0.58), providing additional evidence for its biological relevance.

233
234 We compared our association results for aortic areas with those reported for aortic diameters in
235 recent preprints^{30,31} based on the same UK Biobank imaging dataset, but using different methods
236 and metrics for aortic dimensions. We replicated 73 of the previously reported genome-wide
237 significant association loci and added associations for two clinically relevant phenotypes (ascending
238 and descending aortic distensibility) to identify a further 31 novel associations. Only four of the
239 previously reported SNPs did not replicate. Inspection of the loci for SNPs that were significant in
240 the analysis by Pirruccello et al³⁰, but not in our own, generally showed SNP p-value signals near the
241 genome-wide significance threshold ($p < 5 \times 10^{-8}$) in our analysis. The small differences between
242 associations in the two studies could arise from differences in the methods used to generate
243 quantitative phenotypes or from the differences in participant exclusions between the two studies
244 (for example, we excluded data from participants with known diagnoses of aortic disease and those
245 who were extreme phenotypic outliers).

246

247 Novel aortic loci associated with AAdis included lead SNPs rs7638565 near *ADAMTS9*, which is a
248 significant eQTL for this gene in aorta ($p=5.7 \times 10^{-7}$, NES= -0.22) and rs835341, intronic in *GPX7* and
249 a strong eQTL in the aorta ($p=3 \times 10^{-95}$, NES= -0.92). A novel locus associated with descending
250 aortic distensibility included lead SNP rs112009052, an sQTL for *LTBP4* in fibroblasts ($p=9.6 \times 10^{-67}$,
251 NES= 2.9) but not in aortic tissues that has relevance here due to this gene's role in the TGF- β
252 pathway.

253

254 We identified 21 novel associations with aortic areas including lead SNPs in *KALRN* and *COL21A1*
255 associated with ascending aortic areas and SNPs at loci tagging *AFAP1*, *FGF5/BMP3*, *NOX4*, *FES*
256 and *GATA5/LAMA5* associated with descending aortic areas (see Supplementary Figures S5).

257

258

259 **Sex-specific aortic trait GWAS analyses**

260 We undertook sex-specific GWAS analysis of the area phenotypes. We did not perform these
261 analyses for distensibility phenotypes due to lack of power with the smaller cohort sizes. We
262 contrasted associations discovered for the men and women (numbers of whom were well-balanced
263 in the cohort) using a z test. There were 18 loci (ten for AAmin and eight for DAmin) at which the
264 differences between sexes were significant (adjusted $p < 0.05$). Seven of these associated loci were
265 not significant even at $p < 0.05$ for one sex, despite reaching genome-wide significance ($p < 5 \times 10^{-8}$) for
266 the other (see Table 2). Amongst these sex-specific loci were rs28699256, a missense variant in
267 *ADAMTS7* associated with ascending aortic area in females, but not males (see Table 2; z-test for
268 sex difference, $p=7.6 \times 10^{-4}$). This variant in *ADAMTS7* is in strong LD with the lead SNP associated
269 with AAmin in the full cohort at genome-wide significance (rs7182642; $R^2=0.76$, $D'=0.94$). Amongst
270 the other sex-specific signals were four others with functional data supporting potential biological
271 roles in the aorta, all of which were significant only in males: rs72765298 in *SCAI*, a strong eQTL in
272 aorta (see Table 2; p value for eQTL in aorta= 8.9×10^{-18} , NES= -0.48); rs632650, a significant eQTL
273 for *ALDH2* in aorta (see Table 2; p value for eQTL in aorta= 3.3×10^{-12} , NES= 0.26); rs6573268,
274 associated with DAmin, in *CCDC175* which is a significant eQTL for this gene and others in the aorta
275 (see Table 2; p value for eQTLs in aorta: for *CCDC175* $p=1.2 \times 10^{-6}$, NES = 0.35; for *RTN1* $p=2.4 \times 10^{-7}$,
276 NES= 0.33 and for *L3HYPDH*, $p=1.1 \times 10^{-4}$, NES= 0.25); and rs35346340 in *FES*, a strong eQTL
277 for this gene in aorta (see Table 2; p value for eQTL in aorta 2.4×10^{-15} , NES= 0.3).

278

279 An association with rs12663193 (intronic in *ESR1*) reached genome-wide significance only in
280 females. However, the sex difference was not significant (z-test p value = 0.06).

281

SNP	Gene	Trait	Effect allele	Males			Females			Comparison		
				pval	beta	SE	pval	beta	SE	sig	z stat	z.pval
rs72765298	SCAI	AAmin	T	7.10E-09	15.54	2.68	0.43	1.77	2.25	M	5.58	2.43E-08
rs28699256	ADAMTS7	AAmin	T	0.066	-3.32	1.81	4.10E-09	-8.92	1.52	F	3.37	7.63E-04
rs632650	ACAD10	DAmin	G	1.30E-09	-6.76	1.11	0.54	-0.52	0.85	M	-6.33	2.39E-10
rs6573268	CCDC175	DAmin	G	1.10E-08	5.15	0.90	0.29	0.72	0.69	M	5.53	3.22E-08
rs35346340	FES	DAmin	G	8.10E-09	4.93	0.86	0.081	1.14	0.65	M	5.00	5.62E-07
rs9449999	TBX18	DAmin	A	2.70E-08	-4.52	0.81	0.12	-0.96	0.62	M	-4.94	7.64E-07
rs577351796	TBC1D12	DAmin	C	0.11	-6.50	4.08	6.00E-11	-19.90	3.04	F	3.74	1.83E-04

282

283 **TABLE 2: Lead SNPs at sex-specific loci.** SNPs are shown if they reach genome-wide
 284 significance ($p < 5 \times 10^{-8}$) in one sex and are not significant ($p > 0.05$) in the other. Gene = nearest
 285 gene. Trait = aortic trait with which association in one sex is genome-wide significant, pval = p value
 286 from sex-specific GWAS, beta= effect size from sex-specific GWAS, SE= standard error from sex-
 287 specific GWAS, sig = which sex the SNP has reached genome wide significance in, z stat = z
 288 statistic for comparison between sexes, z.pval= p value of sex comparison.

289

290

291 **Gene-based analysis and tissue specificity**

292 We prioritized potentially causal genes at significant loci using two complementary strategies:
 293 FUMA³², which integrates positional mapping, eQTL associations and HiC-derived 3D chromatin
 294 interactions (see Methods) and MAGMA³³, which aggregates SNP associations within genes. In
 295 total, FUMA identified 973 candidate genes across the six phenotypes, including 390 protein-coding
 296 genes, 164 pseudogenes, 129 lincRNAs, 115 antisense RNAs and 46 miRNAs (Supplementary
 297 Figure S9). MAGMA identified 391 candidate genes with an FDR < 0.01 (Supplementary Figure
 298 S10). The most significant gene associations (MAGMA) for ascending and descending aortic
 299 distensibilities are shown in Table 3.

300

301 Four genes (*MASP1*, *PI15*, *PLCE*, *TBC1D12* [the last likely tagging the *PLCE1* locus]) reached
 302 significance for all 6 aortic traits, with *ELN* at genome-wide significance in all traits except for
 303 DAMax, where it was just below the genome-wide significance threshold.

304

305 Tissue specificity analysis in MAGMA for genes associated with each phenotype demonstrated that
 306 these were significantly enriched for expression in aorta and in coronary artery (p value for
 307 enrichment < 1×10^{-3} in all traits), supporting the validity of our results. See Supplementary Figure
 308 S11 for further details.

309

310

311

AA distensibility						DA distensibility					
CHR	START	STOP	ZSTAT	P (adj)	SYMBOL	CHR	START	STOP	ZSTAT	P (adj)	SYMBOL
1	52870236	52886511	5.01	2.68E-07	PRPF38A	2	20883788	21022882	5.6592	7.61E-09	C2orf43
1	52873954	53019159	4.65	1.67E-06	ZCCHC11	3	186935942	187009810	6.3839	8.63E-11	MASP1
1	53068044	53074723	4.96	3.60E-07	GPX7	5	95726119	95769847	4.0163	2.96E-05	PCSK1
3	37027357	37034795	4.52	3.14E-06	EPM2AIP1	7	73442119	73484237	4.4229	4.87E-06	ELN
3	123798870	124445172	4.85	6.25E-07	KALRN	8	75512010	75735548	4.0596	2.46E-05	RP11-758M4.1
4	146678779	146859787	4.60	2.14E-06	ZNF827	8	75736772	75767264	4.3374	7.21E-06	PI15
5	81575281	81682796	4.68	1.40E-06	ATP6AP1L	8	92114060	92231464	5.0794	1.89E-07	LRRRC69
5	95726119	95769847	6.11	5.00E-10	PCSK1	8	122624356	122653630	4.6601	1.58E-06	HAS2
5	122424816	122529960	5.10	1.69E-07	PRDM6	9	116638562	116818871	4.6059	2.05E-06	ZNF618
6	12290596	12297427	4.72	1.18E-06	EDN1	10	95753746	96092580	7.3635	8.96E-14	PLCE1
7	73442119	73484237	7.11	5.85E-13	ELN	10	96162261	96295687	5.8888	1.95E-09	TBC1D12
8	38585704	38710546	4.58	2.38E-06	TACC1	10	96305547	96373662	5.2578	7.29E-08	HELLS
8	75512010	75735548	5.26	7.03E-08	RP11-758M4.1	11	61535973	61560274	4.2122	1.26E-05	TMEM258
8	75736772	75767264	6.13	4.27E-10	PI15	12	33527173	33592754	4.8085	7.60E-07	SYT10
8	122624356	122653630	6.11	5.00E-10	HAS2	12	38710380	38717784	4.4827	3.69E-06	ALG10B
10	95753746	96092580	5.22	9.07E-08	PLCE1	12	57489191	57525922	4.3707	6.19E-06	STAT6
11	69924408	70035634	5.15	1.34E-07	ANO1	12	94071151	94288616	4.6778	1.45E-06	CRADD
12	21950335	22094336	5.58	1.19E-08	ABCC9	14	92335756	92414331	5.5917	1.12E-08	FBLN5
12	57489191	57525922	5.26	7.24E-08	STAT6	15	32737307	32747835	4.6319	1.81E-06	GOLGA80
15	71389291	72075722	5.27	7.01E-08	THSD4	15	74218330	74244478	4.3266	7.57E-06	LOXL1
15	78916461	79020096	4.96	3.47E-07	CHRN4	15	91426925	91439006	4.7615	9.61E-07	FES
16	75327596	75467383	4.83	6.82E-07	CFDP1	16	75327596	75467383	6.6103	1.92E-11	CFDP1
16	75446582	75498604	4.59	2.19E-06	RP11-77K12.1	16	75446582	75498604	6.2293	2.34E-10	RP11-77K12.1
16	88941266	89043612	5.06	2.12E-07	CBFA2T3	16	75476952	75499395	6.0227	8.58E-10	TMEM170A
16	89006197	89017932	5.07	1.98E-07	RP11-830F9.6	16	75510949	75529282	4.8918	4.99E-07	CHST6
17	1957448	1962981	5.39	3.45E-08	HIC1	16	89724210	89737680	4.1797	1.46E-05	SPATA33
17	1963133	2207065	8.24	8.86E-17	SMG6	17	1963133	2207065	6.0905	5.63E-10	SMG6
17	2206677	2228554	7.68	7.83E-15	SRR	17	2206677	2228554	5.3263	5.01E-08	SRR
17	2225797	2240801	5.33	4.80E-08	TSR1	19	39138289	39222223	5.3381	4.70E-08	ACTN4
20	47240790	47444420	4.61	2.04E-06	PREX1	19	39220827	39260544	4.6378	1.76E-06	CAPN12

312

313 **TABLE 3:** Most significant 30 genes associated with ascending and descending aortic distensibility
314 (MAGMA). P values are converted to adjusted p-values (FDRs) using the Benjamini-Hochberg
315 procedure.

316

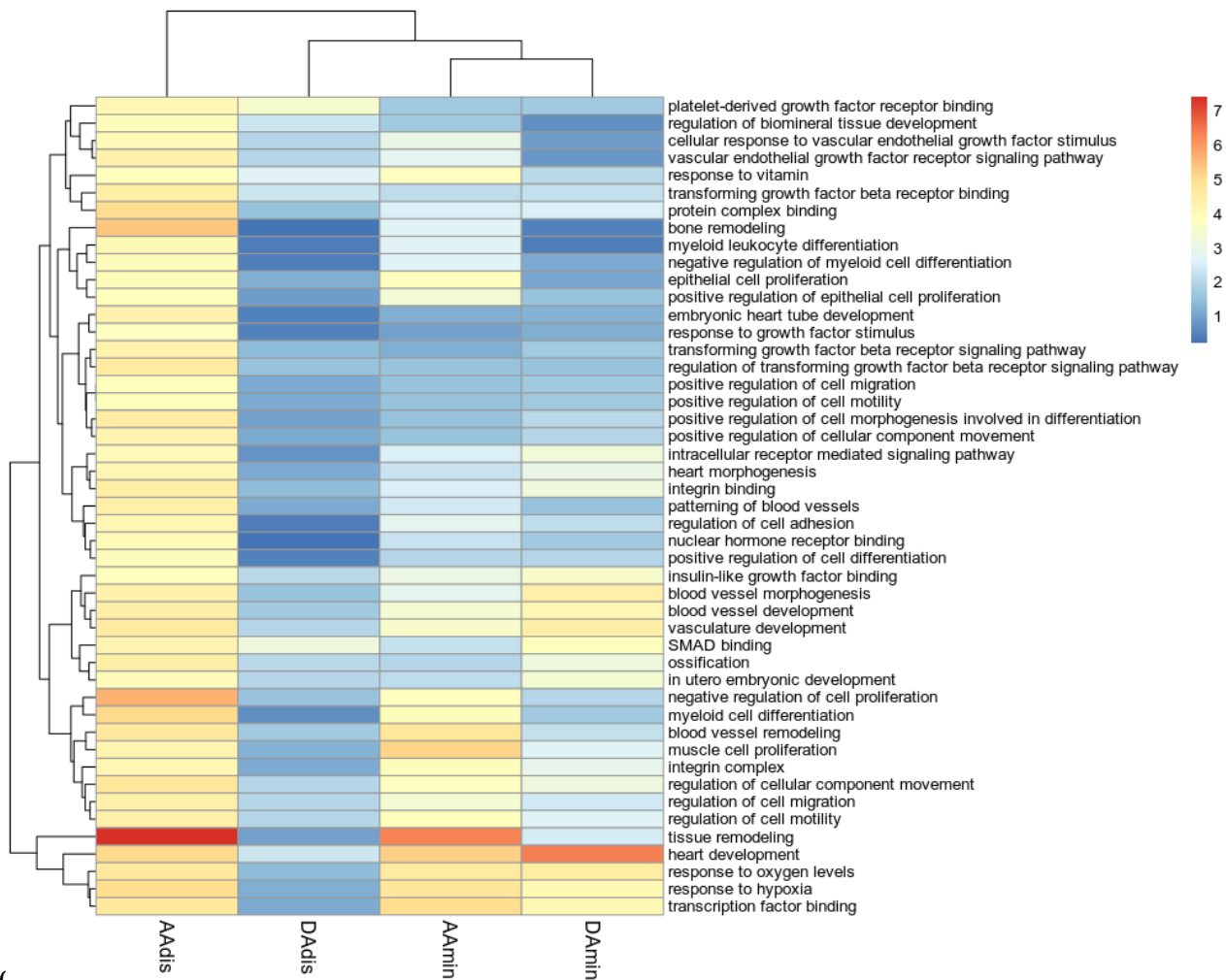
317 **Gene set enrichment and pathways analyses**

318 The GO terms identified by MAGMA (Supplementary Figure S12) that were most significantly
319 associated with our aortic phenotypes highlighted processes important for the development of aortic
320 aneurysms and dissection, such as “extracellular matrix structural constituent” and “smooth muscle
321 contraction”, as well as GO terms related to cardiovascular development.

322

323 DEPICT implicated similar ontologies and identified three molecular pathways significantly enriched
324 in our data (FDR<0.01) for at least one aortic trait (see Figure 2) and of nominal significance in all
325 other traits: regulation of TGF- β signalling (AAdis nominal p value=2.76x10⁻⁵; FDR <0.01), IGF
326 binding (AAdis nominal p value 1.47x10⁻⁴; FDR <0.01) and PDGF binding (AAdis nominal p value

327 7.19×10^{-5} ; FDR <0.01). VEGF signalling was significantly associated with ascending aortic
 328 distensibility (AAdis nominal p value 5.15×10^{-5} ; FDR <0.01).
 329



332 **FIGURE 2: Heatmap of significantly enriched gene ontologies (GO terms) for minimum area**
 333 **and distensibility phenotypes generated by DEPICT.** Colour scale denotes the significance of
 334 enrichment, -log₁₀ scale. Only GO terms significantly enriched in association with AAdis
 335 (FDR<0.01) are presented.
 336

337

338 **Co-expression network analyses**

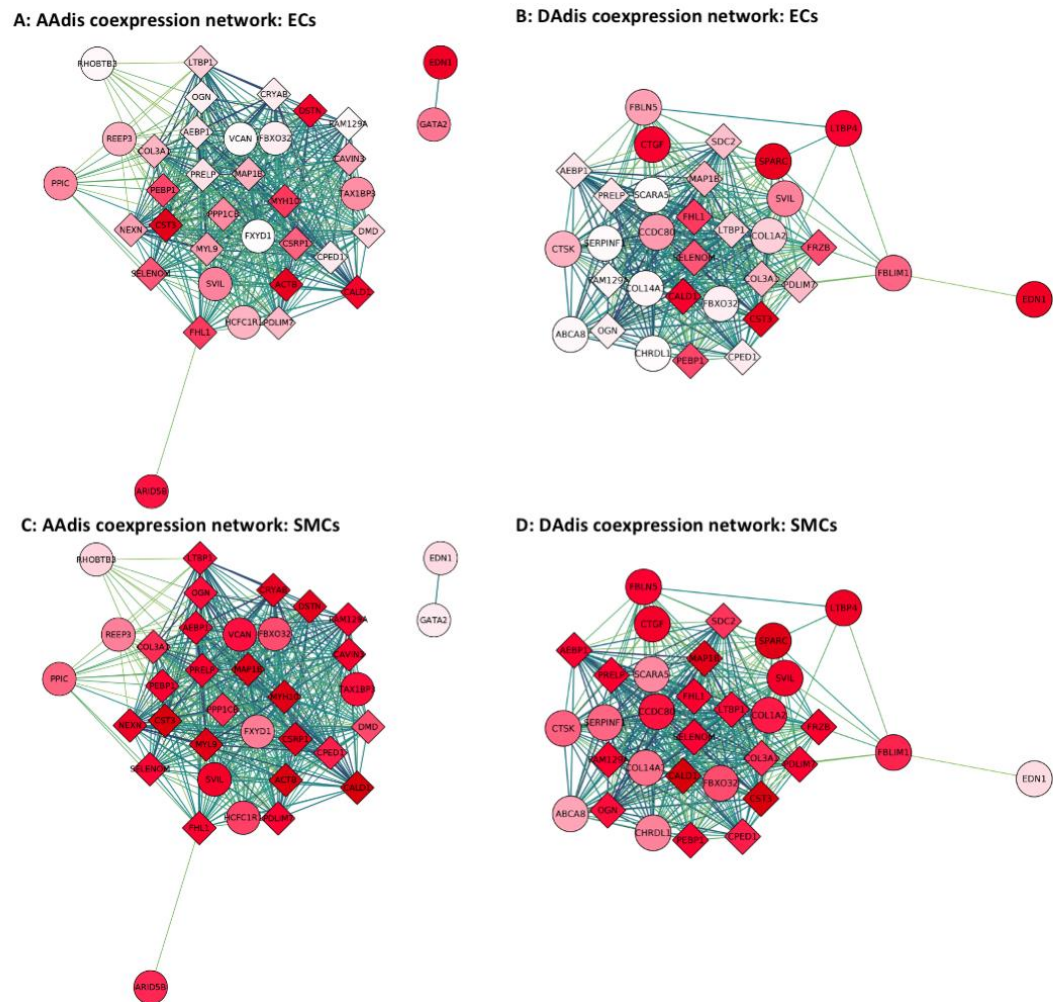
339 Using expression data from single cell transcriptomics of the primate aorta³⁴, we generated co-
 340 expression modules for aortic endothelial and aortic smooth muscle cells. Using our MAGMA (adj. p-
 341 value <0.01) and FUMA gene-based associations (see Methods), we generated functional sub-
 342 networks for each aortic trait, highly enriched for our significant genes and identified hub genes for
 343 modules expressed in aortic endothelial cells and aortic smooth muscle (see Figure 3 and
 344 Supplementary Figures S13-S16). These hub genes include genes involved in smooth muscle cell

345 contraction and differentiation (e.g., *ACTB*, *MYH10*, *MYL9*, *NEXN*, *ARID5B* and *SVIL*), as well as
 346 others associated with TGF- β signalling. In endothelial cells, hub genes identified included *EDN1*
 347 and *GATA2*.

348

349 We used these co-expression modules for pathway analyses as described in Methods. The
 350 importance of extracellular matrix, vascular smooth muscle cell contraction and developmental
 351 pathways were highlighted by enrichment of GO biological pathway and molecular function terms
 352 (e.g. extracellular matrix organisation, collagen-containing extracellular matrix, contractile fibre,
 353 muscle contraction, actin binding, myosin binding, cardiovascular system development). GO terms
 354 related to the TGF- β pathway were also significantly enriched in functional modules derived from
 355 gene associations with all the aortic phenotypes (FDR<0.05).

356



357

358 **FIGURE 3:** Co-expression networks for aortic distensibility GWAS genes generated with primate
 359 single cell expression data for the aorta³⁴. The co-expression networks were derived from extended
 360 models ($r>0.2$) in aortic endothelial (AoECs) and aortic smooth muscle cells (AoSMCs). Round
 361 circles represent genes which were significantly associated with an aortic trait in the current GWAS.
 362 Diamonds represent other genes significantly co-expressed in the published single cell data for the

363 cell-type indicated. The deeper the shade of red, the higher the level of expression of that gene in
364 the specified cell-type. The strength of co-expression is denoted by the colour of the lines joining
365 genes with higher correlations indicated by darker lines. “Hub genes” are found in the centres of
366 these modules. See Supplementary Figures S13-S16 for further co-expression results.

367

368 ***Phenome-wide association studies and MR-PheWAS***

369 We performed a Phenome Wide Association Study (PheWAS) and a subsequent Mendelian
370 Randomisation – Phenome Wide Association Study (MR-PheWAS) to explore associations between
371 our aortic traits of interest and clinical diagnoses in the whole UK Biobank population for which
372 relevant clinical data were available (n= up to 406,827), controlling for age and sex.

373

374 Initial PheWAS identified significant phenotypic associations between aortic traits and multiple
375 hypertension-related clinical codes. Aortic areas showed a positive phenotypic association with
376 hypertension (for example, AAmin $\beta=0.001$; $p=2.5 \times 10^{-21}$). Aortic distensibility was negatively
377 associated with hypertension ($\beta=-0.217$; $p=1.65 \times 10^{-25}$). There was a significant negative association
378 for all traits with type II diabetes mellitus.

379

380 A subsequent analysis of genotypic associations using MR-PheWAS supported a significant causal
381 relationship between AAdis (MTAG) and aortic aneurysms (Inverse Variance Weighted (IVW)
382 OR=0.28, 95% CI 0.16-0.50; p value 2.14×10^{-5} ; consistent directions of effect with Weighted Median
383 (WM)/MR Egger and with use of the single trait analysis of AAdis as the genetic instrument, though
384 the latter did not reach significance), suggesting clinical meaningfulness of the distensibility
385 phenotype. MR-PheWAS also suggested that ascending and descending aortic areas are causally
386 related to the risk of aortic aneurysms without evidence of significant pleiotropy.

387

388 ***Relationship between blood pressure and aortic dimensions***

389 We tested further for bi-directional causal relationships between quantitative blood pressure traits
390 (using GWAS summary statistics from a previous study³⁵) and aortic areas using Mendelian
391 randomisation (MR). MR results supported a bidirectional causal relationship between ascending
392 aortic areas and diastolic blood pressure (DBP; AAmin->DBP; $\beta_{IVW}=0.004$, $p=4.3 \times 10^{-16}$; DBP-
393 >AAmin: $\beta_{IVW}=6.6$; $p=2.5 \times 10^{-5}$) and between ascending aortic area and pulse pressure (PP; AAmin-
394 >PP: $\beta_{IVW}=-0.007$; $p=7.1 \times 10^{-15}$; PP-> AAmin: $\beta_{IVW}=-8.1$, $p=4.4 \times 10^{-7}$). MR-Egger estimates were
395 consistent for all but the DBP-> AAmin analysis, for which the estimates were in the opposite
396 direction. Contamination mixture MR (MR-ConMix, see Methods) showed consistent findings for all
397 analyses. Similar analyses for causal relationships with blood pressure were not performed for
398 distensibility since blood pressure is used for calculation of the trait .

399

400 ***Genetic relationships between aortic traits and cerebral small vessel disease or cervical***
401 ***artery dissection***

402 We explored genetic correlations and potential causal relationships between aortic traits and brain
403 SVD estimated from the brain MRI measure of white matter hyperintensity (WMH) burden. Using
404 LDSC, we identified a significant genetic overlap between all aortic traits and WMH burden which
405 defined a positive association with minimum aortic area and an inverse association for the
406 distensibility measures (AAmin $r_g=0.20$, $p=0.001$; DAmin $r_g=0.22$, $p=2.19 \times 10^{-5}$; AAdis $r_g=-0.22$,
407 $p=5.0 \times 10^{-4}$; DAdis $r_g=-0.33$; $p=1.0 \times 10^{-4}$). In further analyses we found no significant genome-wide
408 overlap between aortic traits and risks of cervical artery dissection, a leading cause of stroke in
409 young people which was associated with aortic phenotypes in an earlier study³⁶. However, the
410 regional level overlap estimates from a Bayesian pairwise GWAS (GWAS-PW) suggest a high
411 probability of shared variants between aortic distensibility traits and the cervical artery dissection
412 (CeAD) risk locus *PHACTR1-EDN1*. Most of the other CeAD risk loci with high probability of shared
413 variants with aortic traits harbour single nucleotide variants (SNVs) associated at genome-wide
414 significance with one or more of the aortic traits. Exceptions to this include regions at chromosomes
415 12 (including *c12orf49*, *RNFT2*, *PAWR*, *OTOGL*), 16 (including *CMIP*, *PKD1L2*, *BCO1*) and 2
416 (including *MBD5*, *EPC2*, *LYPD6B*), suggesting further novel biologically relevant associations with
417 aortic traits in these regions.

418

419 ***Exploring relationships between aortic traits and white matter hyperintensity burden using***
420 ***Mendelian randomisation***

421 A lower aortic distensibility or a greater ascending aortic area is genetically correlated with increased
422 burden of WMH in our data. We hypothesised that there might be a causal relationship between
423 these aortic traits and cerebral small vessel disease. Although a two-sample MR using genetic
424 associations with aortic traits as the instrumental variable and WMH as the outcome showed no
425 evidence for a causal association for any of the aortic traits after FDR correction, after accounting for
426 the effect of blood pressure (either systolic or pulse pressure) using a multivariable MR, we found
427 evidence for a direct causal effect of both ascending and descending aortic distensibility and
428 ascending aortic area on WMH burden. Lower distensibility and higher area were associated with
429 an increased WMH burden (for AAdis $\beta=-0.12$, $p=1.49 \times 10^{-3}$ and DAdis $\beta=-0.21$, $p=1.14 \times 10^{-3}$ using
430 MTAG-derived associations as the instrumental variable and for AAmin $\beta=3.8 \times 10^{-4}$, $p=2.91 \times 10^{-3}$
431 using stage 1 associations as the instrumental variable).

432

433

434 **DISCUSSION**

435 Our analysis provides a first large-scale GWAS of ascending and descending aortic distensibilities,
436 and adds substantively to the literature concerning the genetic basis of variation in aortic
437 dimensions. We show that aortic distensibility has a significant heritable component, with 11% of
438 the variance in AA distensibility and 10% of the variance in DA distensibility explained by the
439 common genetic variants included in our study (increasing to 24% and 21% respectively for the
440 MTAG analysis). We identify 38 loci associated with these measures of aortic stiffness, and a total of
441 31 novel loci for aortic traits including aortic areas (102 loci overall). Annotation of these loci
442 provides evidence for mechanistic associations of TGF- β , IGF, PDGF and VEGF signalling
443 pathways with aortic distensibility.

444
445 The clinical significance of our findings is suggested by the potential causal associations between
446 AAdis (and other aortic traits) and aortic aneurysms defined by MR-PheWAS. Multivariable MR
447 provides new evidence for possible mechanistic associations between cerebral small vessel disease
448 and both aortic distensibilities and aortic area, helping to explain their long-recognised clinical
449 relationships^{20, 37}.

450
451 Mendelian aortopathy or cardiovascular disease associated genes *ELN*³⁸, *THSD4*³⁹, *FBLN5*^{40, 41},
452 *PRDM6*⁴² and *ABCC9*⁴³ directly overlap loci associated with aortic distensibility phenotypes and thus
453 are strong candidates for expression of functional effects of variation at the corresponding
454 loci. Similarly, Mendelian disease genes *FBN1*⁴⁴, *MYH7*⁴⁵, *TBX20*⁴⁶, *MASP1*⁴⁷ and *LOX*⁴⁸ overlap loci
455 associated with aortic area phenotypes. Other genes associated with aortic area in our analyses
456 have previously been associated with risks of acute aortic dissection (*ULK4*, *LRP1*⁴⁹). Several gene
457 ontologies were associated with our measured aortic traits which are also of significance in
458 Mendelian aortic disease⁵⁰. Those GO terms related to the extracellular matrix, cardiovascular
459 development and vascular smooth muscle cell function (with genes such as *ELN*, *ABCC9*, *ANO1*
460 and *PRDM6* associated with AAdis) were amongst the most consistently identified. This overlapping
461 genetic landscape of distensibility (and aortic areas) and aortic aneurysms, and our finding of a likely
462 causal link between these phenotypes using MR-PheWAS suggest that functional pathways related
463 to genes associated with quantitative aortic traits contribute to the pathogenesis of aortic disease.
464 Together, these observations also support the growing consensus that cardiovascular disease
465 phenotypes may be expressed as a result of extremes of normal genetic variation in the
466 population⁵⁹, and support the use of distensibility to predict both aneurysm formation and
467 progression⁴.

468
469 Our data also support a role for TGF- β signalling in determining aortic distensibility in the general
470 population. The TGF- β pathway has long been recognised as an important modulator of aortic

471 function, with variants in many of the major components identified as causal in Mendelian aortic
472 disease such as Loeys-Dietz syndrome⁵¹. Gene ontologies and cell-specific co-expression modules
473 associated with the measured aortic traits suggest that IGF, PDGF and VEGF signalling also play
474 significant roles in aortic biology. The roles of insulin and of insulin-like growth factor signalling are of
475 considerable therapeutic interest for aortic pathology given recent evidence suggesting that
476 metformin, a known regulator of both signalling pathways⁵⁴, could be an effective treatment for
477 abdominal aortic aneurysm, and the consequent initiation of clinical trials testing this^{55,56}.

478

479 Each of these gene sets offers interesting candidates in the search for new Mendelian aortic disease
480 genes. Our results also add to the literature on sex differences in the genomic regulation of
481 cardiovascular traits^{57,58}, with new evidence presented here suggesting distinct, biologically relevant
482 associations in males and females and implicating genes such as *ADAMTS7*, *SCAI*, *ALDH2* and
483 *FES* as sex-specific determinants of aortic traits and thus possibly also the related diseases.

484

485 The strongest SNV association with ascending aortic distensibility was found in close proximity and
486 upstream of *ELN*, the gene encoding elastin, a functionally central component of aortic elastic fibres.
487 *FBLN5* was strongly associated with DAdis. This encodes fibulin-5, another key extracellular matrix
488 protein and a mediator of elastic fibre assembly⁶³. Variants in *FBLN5* cause a Mendelian form of
489 *cutis laxa* associated with aortic aneurysm, vascular tortuosity and supraaortic stenosis^{40,41}.
490 The importance of extracellular matrix (ECM) composition and regulation is also demonstrated by
491 the identification of multiple ECM-related GO terms associated with aortic phenotypes. Specific gene
492 associations also serve to emphasise this, including three members of the ADAMTS family, which
493 regulate ECM turnover: *ADAMTS7* and *ADAMTS8*, both previously associated with aortic minimum
494 areas and replicated here, and a novel association of ascending aortic distensibility with *ADAMTS9*.
495 The strong association of AAdis with *HAS2* (encoding a hyaluronan synthetase) demonstrated that
496 glycosaminoglycan components of the ECM are also key determinants of aortic traits.

497

498 Other specific associations provide insights into the complexity of aortic biology. For example, the
499 second most significant association with AAdis is within a long, non-coding RNA (lncRNA) just 3' of
500 *PCSK1*, a proprotein convertase whose substrates include many hormones such as renin, insulin
501 and somatostatin (associated previously with body mass index and obesity⁶⁴) and therefore which
502 may mediate multiple endocrine influences on aortic traits. The third most significant locus
503 associated with AAdis was previously associated with coronary artery disease⁶⁵ and spans *SMG6* (a
504 regulator of nonsense mediated decay) and *SRR*, a serine racemase. The causal gene at this locus
505 is thought to be *SMG6*, although functional data demonstrating strong eQTLs for *SRR* in all the risk
506 alleles identified suggests it remains a candidate gene for this locus.

507

508 The shared genetic basis of ascending and descending distensibilities is limited (Supplementary
509 Figure 4), consistent with the differing developmental origins of these parts of the aorta, and
510 associated differences in structures of the aortic wall, in which elastin content diminishes more
511 distally⁶⁶. The most significant association for descending aortic distensibility is in *PLCE1*, a gene
512 previously associated with blood pressure traits^{35,67}. Evidence from knockout mice suggests that
513 *PLCE1* contributes to the integration of β -adrenergic signalling with inputs from IGF-1 and other
514 pathways to regulate cardiomyocyte differentiation and growth. We speculate that it might play a
515 similar integrative role in the development and remodelling of aortic tissues.

516 Associations between aortic traits and brain small vessel disease have long been recognised, but
517 the mechanisms responsible have not been defined clearly^{20,68}. This has been a particularly difficult
518 relationship to untangle, as both are subject to confounding influences of blood pressure and other
519 pleiotropic factors. Our multivariate MR provides novel evidence suggesting that aortic traits
520 including distensibility are causally linked to WMH and that this relationship is independent of (and
521 additive to) the effects of blood pressure. By inference, as WMH burden predicts cognitive decline
522 and dementia (with evidence supporting a causal association with Alzheimer type dementia^{16,37}),
523 these results indirectly suggest that aortic stiffening could also contribute to cognitive decline and
524 dementia, e.g. through altered haemodynamics and resultant changes in cerebral blood flow leading
525 to effects on brain endothelial cell function and small vessel remodelling^{69,70}.

526 A shared genomic influence on aortic distensibility and cervical artery dissections was identified at
527 the *PHACTR1/EDN1* locus. Previously, this locus was implicated in coronary artery disease⁷¹,
528 myocardial infarction⁷², migraine⁷³, fibromuscular dysplasia⁷⁴ and cervical artery dissection⁷⁵. We
529 demonstrated an association of *EDN1* with ascending aortic distensibility, and further characterised
530 *EDN1* as a hub gene in co-expression networks derived from aortic endothelia, suggesting that
531 *EDN1* may be responsible for (or functionally contribute to) this shared genetic association with both
532 CeAD risk and aortic distensibility,

533 Although we have made several novel observations, there are obvious limitations of our study. The
534 GWAS was restricted to the analysis of Caucasian individuals, and so the generalisability of our
535 results for people from other ethnic backgrounds is uncertain. Second, the accuracy (and possibly
536 also the precision) of the distensibility measures likely was reduced by the need to use non-invasive
537 blood pressure measurements (acquired on the same day as the imaging) as proxies for central
538 blood pressure recordings. The ascending and descending aortic distensibility measures also suffer
539 from confounding due to a likely bidirectional relationship with blood pressure, given the use of blood
540 pressure indices in the derivation of the phenotype. Uncontrolled confounding from residual effects
541 of blood pressure could bias the Mendelian randomization analyses. Nevertheless, our genetic

542 associations were significantly enriched for genes expressed in the aorta and identify genes known
543 to be important in aortic biology, affording some confidence in the robustness of our results.

544

545 In summary, our results provide genetic association data highlighting roles for TGF- β and other
546 growth factor (IGF, PDGF, VEGF) signaling pathways in the elastic function of the aorta and, by
547 inference, in aortic disease. We present new evidence for potential causal links between lower
548 aortic distensibility and increased risk of aortic aneurysm and for common causal mechanisms
549 relating cerebral small vessel disease and aortic structure and function that could explain the
550 clinically observed relationships between late life cognitive decline and aortic disease^{14, 18}. Better
551 understanding of the underlying mechanisms based on these genetic data could lead to the
552 identification of new therapeutic targets for reduction of both cardiovascular disease and dementia
553 risks.

554

555

556 **METHODS**

557

558 ***Data***

559 The UK Biobank cardiac magnetic resonance imaging (CMR) was conducted using a rigorously
560 controlled acquisition protocol⁷⁶. The mean age at the time of CMR was 64 ± 8 years (range 45–82,
561 49% of participants were male). Exclusion criteria for imaging included a range of relative
562 contraindications to magnetic resonance imaging scanning as well as childhood onset disease and
563 pregnancy. Aortic cine images were acquired using transverse bSSFP sequence at the level of the
564 pulmonary trunk and right pulmonary artery on clinical wide bore 1.5 Tesla scanners (MAGNETOM
565 Aera, Syngo Platform VD13A, Siemens Healthcare). Each cine image sequence consists of 100
566 time frames. The typical image size is 240x196 pixel with the spatial resolution of
567 1.6×1.6 mm². Brachial blood pressure was obtained using a manual sphygmomanometer and
568 converted into central blood pressure for the distensibility calculations by applying a brachial-to-
569 aortic transfer function using the Vicorder software⁷⁶.

570

571

572 ***Derivation of imaging phenotypes***

573 A recurrent convolutional neural network was developed for aortic image segmentation and trained
574 using manual annotations of 800 ascending aorta and descending aorta images (400 subjects and 2
575 time frames per subject)^{25, 27}. The network was applied to segmenting aortic images across the
576 cardiac cycle. A semi-automated quality control was performed for all segmentations, consisting
577 of automated checking of missing or fragmented segmentation and subsequent manual
578 checking on segmentation screenshots. Six aortic imaging phenotypes were calculated based on

579 the automated segmentations, including those for the maximal area, minimal area and distensibility
580 for both the ascending aorta and descending aorta⁴. Distensibility was calculated as

581

$$582 \quad Dis = \frac{A_{max} - A_{min}}{A_{min} \times (SBP - DBP)}$$

583

584 where A_{max} and A_{min} denote the maximal and minimal area and SBP and DBP denote the
585 systolic and diastolic central blood pressure, measured at the imaging visit during the study protocol
586 (measured brachially and converted to central blood pressure by applying a brachial-to-central
587 transfer function as described above). After running the image segmentation pipeline
588 and performing quality control, imaging phenotypes were available for 36,996 participants.

589

590 **Genomic analyses**

591 We performed stage 1 GWAS on six imaging phenotypes (AA_{max} , AA_{min} , DA_{max} , DA_{min} , AA_{dis}
592 and DA_{dis}). Outliers with phenotype values >4 standard deviations (SDs) from the mean were
593 excluded to ensure we did not include patients with undiagnosed aortic aneurysm in our
594 results. After exclusions for image quality control, outlying BMI (<15 or >40), stage IV hypertension,
595 missing covariates, diagnosis of aortic disease and non-white ethnicity, 4,406 participants were
596 excluded leaving 32,590 individuals for the GWAS of AA_{max} , AA_{min} , DA_{max} , and DA_{min} , and
597 29,895 for the GWAS of AA_{dis} and DA_{dis} (the latter figure is lower due to more missing
598 contemporaneous blood pressure recording data and incomplete imaging sets). See Supplementary
599 Figure S1 for more details on exclusions. After exclusions, we rank-normalised the distensibility
600 phenotypes due to the non-normal distribution of the distensibility phenotypes (Supplementary
601 Figure S2). Aortic area phenotypes approximated a normal distribution and so raw areas were used
602 to facilitate interpretation of the effect sizes. The genetic model was adjusted for age at time of
603 imaging, sex, mean arterial pressure, height, and weight. We used the linear mixed model approach
604 implemented in BOLT-LMM (v2.3.4)⁷⁷. The genetic relationship matrix (GRM) constructed by BOLT
605 was based on all directly genotyped SNPs ($N = 340,336$) passing the threshold settings ($MAF >$
606 0.05 , $p(\text{HWE}) > 1e^{-6}$ and genotype calling rate > 98.5). For the main analysis, a threshold of MAF
607 > 0.01 was applied to the SNPs. Genomic inflation (λ) was calculated in R as the median chi
608 square values derived from the p-values divided by the expected median of a chi square distribution
609 with 1 degree of freedom.

610

611 We used MTAG (version 1.0.8)²⁸ for multi-trait analysis of GWAS summary statistics to increase
612 power. MTAG can identify genetic loci associated with a particular phenotype where the single-trait
613 GWAS is underpowered. The method uses the correlation structure of the trait in question with
614 other traits to boost power. It therefore may fail to identify trait-specific loci but will increase power to
615 detect loci associated with the other related and correlated traits. We used all 6 aortic phenotypes

616 for our MTAG analysis. Regression coefficients (beta) and their standard errors were used for
617 MTAG. The results of the multi-trait analyses are shown as Figure 1B and in Supplementary Figures
618 S7-8.

619

620 We additionally conducted a sex-specific analysis by performing GWAS on aortic areas for
621 autosomal SNPs in men and women separately, using the BOLT-LMM pipeline as above, and
622 compared the sizes of the sex-specific genetic associations for SNPs with a P-value smaller than
623 5×10^{-8} using a z-test⁷⁸. We did not repeat this analysis for distensibility phenotypes as it was
624 underpowered because of the reduced cohort size and smaller effect sizes for the distensibility
625 SNPs as well as lower heritability estimates for these traits.

626

627 To classify genomic loci associated with our imaging phenotypes, GWAS summary statistics were
628 processed using FUMA (v1.3.6)³² and a pre-calculated LD structure based on the European
629 population of the 1000 Genome Project⁸². SNPs that reached genome-wide significance ($p < 5 \times 10^{-8}$)
630 and with $r^2 < 0.6$ were defined as independently significant. All variants with $r^2 \geq 0.6$ were labelled as
631 candidate variants for further annotation by FUMA. In a second clumping procedure to define lead
632 SNPs, those correlated with $r^2 < 0.1$ were defined as independently significant. Finally, proximal LD
633 blocks of independent significant SNPs with less than 250kb distance were merged and considered
634 as a single genomic locus. To consolidate genomic loci across different traits, the merge function
635 implemented in bedtools was applied⁷⁹.

636

637 For the association of SNPs with genes, biological processes and tissue expression, we applied the
638 SNP2GENE function implemented in FUMA to the summary SNP statistics. For the positional
639 mapping of SNPs to genes, a maximal distance of 10kb was set. eQTL mapping was performed
640 based on the aorta tissue samples in GTEx v8 using only gene pairs with significant SNPs (with the
641 default settings of FDR < 0.05 or p value < $1e^{-3}$). 3D chromatin interaction mapping was based on
642 HiC aorta data (GSE87112) within a promoter region window of 250bp upstream and 500bp
643 downstream from the transcriptional start site and a threshold for significant loops of FDR < $1e^{-6}$.
644 Enhancer and promoter regions were annotated using the aorta epigenome (E065) from the
645 Roadmap Epigenome Project (<http://www.roadmapepigenomics.org/>). MAGMA (Multi-marker
646 Analysis of GenoMic Annotation) was employed to obtain the significance of individual genes with
647 the specificity of tissue expression based on 54 types in GTEx v8 and the association with 10,678
648 gene sets from MsigDB v6.2 (with 4761 curated gene sets and 5917 GO categories). Further
649 annotation of significant SNPs and loci was performed manually with SNP lookups in GTEx v8²⁹;
650 normalised effect sizes are reported from this dataset using “Artery-Aorta” for the main analysis and
651 including other arterial tissue types (“Artery – Tibial” and “Artery – Coronary”) where stated.

652

653 For Gene Ontology (GO) enrichment analysis, the Data-driven Expression Prioritized Integration for
654 Complex Traits (DEPICT) software was applied (v1 beta rel194, www.broadinstitute.org/depict),
655 which is based on probabilistic memberships of genes across reconstituted gene sets⁸⁰ For LD-
656 based clumping by PLINK⁸¹, which precedes the DEPICT analysis, a p-value threshold of 10^{-5} , a
657 distance threshold of 500kb and a LD threshold of 0.1 was set (following the recommendations on
658 the DEPICT website). Note that DEPICT excludes any SNPs in the HLA region, on a sex
659 chromosome, or not found in the 1000 Genomes Project data.

660

661 Comparisons between our data and those reported by Pirruccello et al³⁰. and Tcheandjieu et
662 al³¹ were made using the lead SNPs and corresponding beta-values. To assess the degree of
663 convergence of their studies with our results, lead SNPs were assigned to a genomic locus found in
664 our study if they were within the locus or a 250kb distance interval.

665

666 **LD Score regression**

667 We performed LD Score regression to assess the heritability of the imaging phenotypes. The
668 genetic correlation between imaging phenotypes and blood pressure by LD score was computed
669 using 1000 Genomes European data⁸². We used the GWAS summary statistics for SBP, DBP and
670 pulse pressure (PP) from the International Consortium for Blood Pressure (ICBP)³⁵ for the
671 corresponding analyses for genetic correlation with blood pressure.

672

673 **Co-expression analysis**

674 Co-expression networks for aortic phenotypes were derived using a single cell RNA-seq (scRNA-
675 seq) data set for primate arteries³⁴. The data were obtained from Gene Expression Omnibus
676 (accession number GSE117715) and included read counts for over 9000 single cells from aortas
677 and coronary arteries of 16 *Macaca fascicularis*. Low abundance genes were removed if they had
678 read counts of less than 5% of the cells, leaving a total of 9903 genes for further analysis. The
679 Bioconductor package *scater* was applied to compute log-transformed normalised expression values
680 from the count matrix⁸³. Subsequently, correlation of expression and its significance was derived
681 using the *correlatePairs* function of the Bioconductor *scran* package, which calculated modified
682 Spearman correlation coefficients and derived their significance using a permutation approach⁸⁴. A
683 basal co-expression network was constructed using gene pairs with significant correlation (FDR <
684 0.01) and a minimum Spearman correlation coefficient *rho* of 0.1 or 0.2. Subsequently, sub-
685 networks for imaging phenotypes were derived by retrieving gene pairs with at least one gene
686 associated by MAGMA or FUMA with the specific phenotype.

687

688 Functional enrichment of genes connected with variants identified on GWAS was carried out using
689 overrepresentation enrichment analysis implemented in the Bioconductor *clusterProfiler* package⁸⁵.

690 The background gene set (or universe) was defined by the genes covered by the scRNA-seq data
691 after exclusion of low abundance genes.

692

693 ***Mendelian randomization (MR)***

694 To investigate potentially causal relationships between aortic phenotypes and diseases, we
695 performed bidirectional two-sample Mendelian randomization (MR) using our GWAS for aortic
696 imaging phenotypes and the International Consortium for Blood Pressure GWAS on blood
697 pressure³⁵. We limited our MR analyses to AAm_{ax}, AA_{min}, DA_{max}, and DA_{min} because blood
698 pressure is included in the calculation of the distensibility measure.

699

700 For either direction of potential causal relationships between the aortic phenotypes and blood
701 pressure, we selected SNPs associated with the exposure at genome-wide significance level (P-
702 value < 5 × 10⁻⁸ and F-statistic > 10). For SNPs correlated with r² greater than 0.1, we used only the
703 SNP with the smallest p-value for the SNP-exposure association. We tested the validity of the
704 genetic variants as instrumental variables using the contamination mixture method (MR-ConMix)⁸⁶.
705 The contamination mixture method constructs a likelihood function based on the SNP-specific
706 estimates and evaluates the SNP-specific contribution to the likelihood.

707

708 In each case, we estimated SNP-specific associations as the ratio of SNP outcome to exposure
709 associations (Wald ratio)⁸⁷. SNP-specific associations were combined using the inverse-variance
710 weighted (IVW) estimator⁸⁸. The putative causal effect (β_{IVW}) of an exposure on a given outcome
711 was estimated using the inverse-variance weighting (IVW) method as the weighted sum of the ratios
712 of beta-coefficients from the SNP-outcome associations for each variant (j) over corresponding beta-
713 coefficients from the SNP-exposure associations (β_j). The ratio estimates from each genetic variant
714 were averaged after weighting on the inverse variance (W_j) of β_j across L uncorrelated SNPs,

715

$$716 \quad \beta_{IVW} = \frac{\sum_{j=1}^L W_j \beta_j}{\sum_{j=1}^L W_j}$$

717

718 We also used weighted median (WM) and MR-Egger regressions as sensitivity methods to test the
719 robustness of associations⁸⁸. Potential horizontal pleiotropic effects were investigated using MR-
720 Egger⁸⁹. Outlier SNPs identified by MR-PRESSO were excluded from the analyses⁹⁰. In an
721 additional analysis, we tested the validity of the genetic variants as instrumental variables using MR-
722 ConMix⁸⁶. We accounted for multiple comparisons of four aortic imaging phenotypes, three blood
723 pressure traits, and two directions using Bonferroni correction with a P-value threshold of
724 0.05/(4*3*2)=0.002

725

726 MR analysis was also used to investigate the potential causal relationships between different aortic
727 traits with WMH. In addition to IVW, WM, and MR-Egger, we implemented R package RadialMR
728 (available through CRAN repositories)⁹¹. A p-value < 0.01 correcting for 6 tests (for the 6 aortic
729 traits) was considered significant. In the presence of heterogeneity ($P_{\text{Het}} < 0.01$, Cochran's Q statistic)
730 due to horizontal pleiotropy, RadialMR was used in the identification of pleiotropic SNPs that have
731 the largest contribution to the global Cochran's Q statistic by regressing the predicted causal
732 estimate against the inverse variance weights. After excluding influential outlier SNPs, the IVW test
733 was repeated along with MR-Egger regression in which the regression model contains the intercept
734 term representing any residual pleiotropic effect⁹². Non-significant MR-Egger intercept was used as
735 an indicator to formally rule out horizontal pleiotropy. Relative goodness of fit of the MR-Egger effect
736 estimates over the IVW approach was quantified using Q_R statistics, which is the ratio of the
737 statistical heterogeneity around the MR-Egger fitted slope divided by the statistical heterogeneity
738 around the IVW slope. A Q_R close to 1 indicates that MR-Egger is not a better fit to the data and
739 therefore offers no benefit over IVW⁹¹.

740

741 ***Multivariable MR***

742 We also conducted multivariable two sample MR (MVMR) to estimate the direct effect of aortic traits
743 on the cerebral small vessel disease (cSVD) outcome (WMH) after accounting for potential
744 confounding with blood pressure traits, by conditioning on every other explanatory variable included
745 in the model. Different combinations of explanatory variables were considered and the F_{TS}
746 conditional on the other variables was calculated as a measure of instrument strength⁹³. Briefly,
747 MVMR by regressing a given instrumental variable on all the remaining variables as controls
748 generates a predicted value for the instrumental variable that is not correlated with other variables in
749 the model thus accounting for possible pleiotropic effects.

750

751 ***MR phenome-wide association studies (MR-PheWAS)***

752 We performed an MR-PheWAS using data from UK Biobank participants who did not undergo aortic
753 imaging to assess the effects of aortic traits on clinical disease classifications. Using the PheWAS
754 package (<https://github.com/PheWAS/PheWAS>), we mapped 1,157 phecodes with more than 200
755 cases from the International Classification of Diseases, 9th Revision, Clinical Modification (ICD-9-
756 CM) and the International Classification of Diseases, 10th Revision, Clinical Modification (ICD-10-
757 CM).⁹⁴ For each aortic imaging phenotype, we selected SNPs with a p-value < 5×10^{-8} and minor
758 allele frequency > 0.05 from the single trait GWAS for AAm_{ax}, AA_{min}, DA_{max}, and DA_{min}, and
759 from the multi trait GWAS for AA_{dis} and DA_{dis}. Given that we considered a large number of
760 phecodes as the outcome in the MR-PheWAS analysis with the number of cases ranging from 201
761 to 116,879 (median=1,353), we used a more stringent LD threshold for independent SNPs ($r^2 < 0.01$)
762 to achieve a better stabilised model. The PheWAS model was adjusted for age, sex, genotype array,

763 and its four principal components for population stratification. MR estimates were then obtained for
764 each pair of aortic traits and phecode by combining the SNP-specific associations using IVW, WM,
765 and MR-Egger. We accounted for multiple comparisons of 1,157 phecodes using Bonferroni
766 correction with $p\text{-value} < 0.05/1,157 = 4.3 \times 10^{-5}$.

767
768 ***Analyses of associations of aortic and cervical artery dissection***

769 LD score regression (LDSR) method was applied to test genetic correlation at the genome-wide
770 scale for the different aortic traits with the most common MRI feature of cSVD, WMH and with
771 cervical artery dissection (CeAD). GWAS summary statistics were obtained from recently published
772 consortia GWAS of cerebral phenotypes (from the CHARGE and CADISP consortia respectively)³⁷,
773 ⁷⁵. For this, common variants, mapping to the Hapmap3 reference panel were employed. As the
774 slope from the regression of the Z-score product from the two GWAS summary statistics on the LD-
775 score gives the genetic covariance, the intercept of the genetic covariance was used as an indirect
776 measure of sample overlap⁹⁵, which corresponds to the average polygenic effects captured by
777 genetic variants spread across the genome. A p-value < 0.006 (adjusting for 8 simultaneous tests)
778 was considered significant.

779
780 LDSR could potentially miss significant correlations at the regional level due to the balancing-
781 effect⁹⁶. A Bayesian pairwise GWAS approach (GWAS-PW) was applied to systematically test for
782 locally correlated regions⁹⁷. The GWAS-PW identified trait pairs with high posterior probability of
783 association (PPA) using a shared genetic variant (model 3, $PPA3 > 0.90$). To ensure that PPA3 is
784 unbiased by sample overlap, fgwas v.0.3.6⁹⁸ was run on each pair of traits and the correlation
785 estimated from regions with null association evidence ($PPA3 < 0.20$) was used as a correction factor.
786 Additionally, to estimate the directionality of associations between trait pairs in regions with
787 $PPA3 > 0.90$, a simple rank-based correlation test was applied. Independence between regions was
788 estimated as proposed by Berisa and Pickrell⁹⁹. Only the most strongly associated variant for the
789 outcome per region showing high PPA3 is reported.

790
791
792
793
794

SUPPLEMENTARY FIGURES

- 795
796
797 Supplementary Figure 1 Exclusions
798 Supplementary Figure 2 Distribution of traits
799 Supplementary Figure 3 Phenotypic correlation between traits
800 Supplementary Figure 4 Genotypic correlation between traits (LDSC)
801 Supplementary Figure 5 All Manhattan plots stage 1 GWAS
802 Supplementary Figure 6 All QQ plots stage 1 GWAS
803 Supplementary Figure 7 All Manhattan plots MTAG
804 Supplementary Figure 8 All QQ plots stage 2 (MTAG) GWAS
805 Supplementary Figure 9 FUMA genes results
806 Supplementary Figures 10 MAGMA genes Manhattan plots
807 Supplementary Figure 11 MAGMA tissue expression
808 Supplementary Figure 12 MAGMA GO heatmap
809 Supplementary Figure 13 Coexpression networks for AAdis
810 Supplementary Figure 14 Coexpression networks for DAdis
811 Supplementary Figure 15 Coexpression networks for AAmin
812 Supplementary Figure 16 Coexpression networks for DAmn

813

814

815

816

ACKNOWLEDGEMENTS

817

818

819

820

821

822

823

824

825

826

827

828

829

830

831

PMM acknowledges generous personal and research support from the Edmond J Safra Foundation and Lily Safra, a National Institute for Health Research (NIHR) Senior Investigator Award, the UK Dementia Research Institute and the NIHR Biomedical Research Centre at Imperial College London. CF acknowledges generous support from the BHF Imperial Centre of Research Excellence RE/18/4/34215. This research has been conducted using the UK Biobank Resource under Application Number 18545. PE is director of the Medical Research Council (MRC) Centre for Environment and Health and acknowledges support from the MRC (MR/L01341X/1; MR/S019669/1). PE is director of the Health Protection Research Unit in Chemical and Radiation Threats and Hazards, funded by the NIHR. PE also acknowledges support from the NIHR Imperial Biomedical Research Centre, the Imperial College British Heart Foundation Centre for Research Excellence (RE/18/4/34215), the UK Dementia Research Institute at Imperial College London (MC_PC_17114), and Health Data Research UK for London. SD is supported by a grant overseen by the French National Research Agency (ANR) as part of the 'Investment for the Future'

832 Programme ANR-18- RHUS-002 and by the ERC and the EU H2020 under grant agreements
833 640643, 667375, and 754517.

834

835 The CADISP study has been supported by Inserm, Lille 2 University, Institut Pasteur de Lille and
836 Lille University Hospital and received funding from the ERDF (FEDER funds) and Région Nord-Pas
837 de Calais in the frame of Contrat de Projets Etat-Region 2007-2013 Région Nord-Pas-de-Calais -
838 Grant N°09120030, Centre National de Genotypage, Emil Aaltonen Foundation, Paavo Ilmari
839 Ahvenainen Foundation, Helsinki University Central Hospital Research Fund, Helsinki University
840 Medical Foundation, Päivikki and Sakari Sohlberg Foundation, Aarne Koskelo Foundation, Maire
841 Taponen Foundation, Aarne and Aili Turunen Foundation, Lilly Foundation, Alfred Kordelin
842 Foundation, Finnish Medical Foundation, Orion Farnos Research Foundation, Maud Kuistila
843 Foundation, the Finnish Brain Foundation, Biomedicum Helsinki Foundation, Projet Hospitalier de
844 Recherche Clinique Régional, Fondation de France, Génopôle de Lille, Adrinord, Basel Stroke-
845 Funds, Käthe-Zingg-Schwichtenberg-Fonds of the Swiss Academy of Medical Sciences, Swiss
846 Heart Foundation.

847

848 **CADISP list of investigators**

849 Belgium: Departments of Neurology, Erasmus University Hospital, Brussels and Laboratory of
850 Experimental Neurology, ULB, Brussels (Shérine Abboud, Massimo Pandolfo); Department of
851 Neurology, Leuven University Hospital (Vincent Thijs). France: Departments of Neurology, Lille
852 University Hospital-Inserm U1171 (Didier Leys, Marie Bodenant), Sainte-Anne University Hospital,
853 Paris (Fabien Louillet, Emmanuel Touzé, Jean-Louis Mas), Pitié-Salpêtrière University Hospital,
854 Paris (Yves Samson, Sara Leder, Anne Léger, Sandrine Deltour, Sophie Crozier, Isabelle Méresse),
855 Amiens University Hospital (Sandrine Canaple, Olivier Godefroy), Dijon University Hospital (Maurice
856 Giroud, Yannick Béjot), Besançon University Hospital (Pierre Decavel, Elizabeth Medeiros, Paola
857 Montiel, Thierry Moulin, Fabrice Vuillier); Inserm U744, Pasteur Institute, Lille (Jean Dallongeville).
858 Finland : Department of Neurology, Helsinki University Central Hospital, Helsinki (Antti J Metso,
859 Tiina Metso, Turgut Tatlisumak); Germany: Departments of Neurology, Heidelberg University
860 Hospital (Caspar Grond-Ginsbach, Christoph Lichy, Manja Kloss, Inge Werner, Marie-Luise Arnold),
861 University Hospital of Ludwigshafen (Michael Dos Santos, Armin Grau); University Hospital of
862 München (Martin Dichgans); Department of Rehabilitation: Schmieder-Klinik, Heidelberg (Constanze
863 Thomas-Feles, Ralf Weber, Tobias Brandt). Italy: Departments of Neurology: Brescia University
864 Hospital (Alessandro Pezzini, Valeria De Giuli, Filomena Caria, Loris Poli, Alessandro Padovani),
865 Milan University Hospital (Anna Bersano, Silvia Lanfranconi), University of Milano Bicocca, San
866 Gerardo Hospital, Monza, Italy (Simone Beretta, Carlo Ferrarese), Milan Scientific Institute San
867 Raffaele University Hospital (Giacomo Giacolone); Department of Rehabilitation, Santa Lucia
868 Hospital, Rome (Stefano Paolucci). Switzerland: Department of Neurology, Basel University Hospital
869 (Philippe Lyrer, Stefan Engelter, Felix Fluri, Florian Hatz, Dominique Gisler, Leo Bonati, Henrik

870 Gensicke, Margareth Amort). UK: Clinical Neuroscience, St George's University of London (Hugh
871 Markus). USA : Department of Neurology, Salt Lake City, USA (Jennifer Majersik); Department of
872 Neurology, University of Virginia, Charlottesville, USA (Bradford Worrall, Andrew Southerland);
873 Department of Neurology, Baltimore, USA (John Cole, Steven Kittner)

874

875

876 **COMPETING INTERESTS/DISCLOSURES**

877 PMM acknowledges consultancy fees from Novartis, Bristol Myers Squibb, Celgene and Biogen. He
878 has received honoraria or speakers' honoraria from Novartis, Biogen and Roche and has received
879 research or educational funds from Biogen, Novartis, GlaxoSmithKline and Nodthera.

880

881

882 **CO-AUTHOR CONTRIBUTIONS**

883 CF, MF, JH, SF, AD and PMM co-designed the study. CF, MF, WB, JH, AP, AR and MS performed
884 quality control and core analyses. SD, EP, JW and PE provided additional methodological
885 guidance. CF, MF, JH, AD and PMM drafted the manuscript. All authors reviewed, contributed to
886 serial revisions and approved the manuscript.

887

888

889

890

891

892

893

894

895

896

897

898

899

900

901

902

903

904

905

906

907

908

909

910

911

912

913

914

915

916

917

918

919

920

921

922

923

924

925

926

927

928

929

930

931

932

933

934

935

936

References

1. Ohyama Y, Redheuil A, Kachenoura N, Ambale Venkatesh B, Lima JAC. Imaging Insights on the Aorta in Aging. *Circulation Cardiovascular imaging*. 2018;11(4):e005617.
2. Teixido-Tura G, Redheuil A, Rodriguez-Palomares J, Gutierrez L, Sanchez V, Forteza A, et al. Aortic biomechanics by magnetic resonance: early markers of aortic disease in Marfan syndrome regardless of aortic dilatation? *International journal of cardiology*. 2014;171(1):56-61.
3. de Wit A, Vis K, Jeremy RW. Aortic stiffness in heritable aortopathies: relationship to aneurysm growth rate. *Heart, lung & circulation*. 2013;22(1):3-11.
4. Nollen GJ, Groenink M, Tijssen JG, Van Der Wall EE, Mulder BJ. Aortic stiffness and diameter predict progressive aortic dilatation in patients with Marfan syndrome. *European heart journal*. 2004;25(13):1146-52.
5. Redheuil A, Wu CO, Kachenoura N, Ohyama Y, Yan RT, Bertoni AG, et al. Proximal Aortic Distensibility Is an Independent Predictor of All-Cause Mortality and Incident CV Events: The MESA Study. *Journal of the American College of Cardiology*. 2014;64(24):2619-29.
6. Mattace-Raso FU, van der Cammen TJ, Hofman A, van Popele NM, Bos ML, Schalekamp MA, et al. Arterial stiffness and risk of coronary heart disease and stroke: the Rotterdam Study. *Circulation*. 2006;113(5):657-63.
7. Ben-Shlomo Y, Spears M, Boustred C, May M, Anderson SG, Benjamin EJ, et al. Aortic pulse wave velocity improves cardiovascular event prediction: an individual participant meta-analysis of prospective observational data from 17,635 subjects. *Journal of the American College of Cardiology*. 2014;63(7):636-46.
8. Cuspidi C, Facchetti R, Bombelli M, Re A, Cairoa M, Sala C, et al. Aortic root diameter and risk of cardiovascular events in a general population: data from the PAMELA study. *Journal of hypertension*. 2014;32(9):1879-87.
9. Kamimura D, Suzuki T, Musani SK, Hall ME, Samdarshi TE, Correa A, et al. Increased Proximal Aortic Diameter is Associated With Risk of Cardiovascular Events and All-Cause Mortality in Blacks The Jackson Heart Study. *Journal of the American Heart Association*. 2017;6(6).
10. Lam CS, Gona P, Larson MG, Aragam J, Lee DS, Mitchell GF, et al. Aortic root remodeling and risk of heart failure in the Framingham Heart study. *JACC Heart failure*. 2013;1(1):79-83.
11. de Roos A, van der Grond J, Mitchell G, Westenberg J. Magnetic Resonance Imaging of Cardiovascular Function and the Brain: Is Dementia a Cardiovascular-Driven Disease? *Circulation*. 2017;135(22):2178-95.
12. van Sloten TT, Protogerou AD, Henry RM, Schram MT, Launer LJ, Stehouwer CD. Association between arterial stiffness, cerebral small vessel disease and cognitive impairment: A systematic review and meta-analysis. *Neurosci Biobehav Rev*. 2015;53:121-30.
13. Qiu C, Winblad B, Viitanen M, Fratiglioni L. Pulse pressure and risk of Alzheimer disease in persons aged 75 years and older: a community-based, longitudinal study. *Stroke; a journal of cerebral circulation*. 2003;34(3):594-9.
14. Raisi-Estabragh Z, M'Charrak A, McCracken C, Biasioli L, Ardissino M, Curtis EM, et al. Associations of cognitive performance with cardiovascular magnetic resonance phenotypes in the UK Biobank. *European heart journal cardiovascular Imaging*. 2021.
15. Moroni F, Ammirati E, Rocca MA, Filippi M, Magnoni M, Camici PG. Cardiovascular disease and brain health: Focus on white matter hyperintensities. *Int J Cardiol Heart Vasc*. 2018;19:63-9.

- 937 16. DeBette S, Schilling S, Duperron MG, Larsson SC, Markus HS. Clinical Significance of
938 Magnetic Resonance Imaging Markers of Vascular Brain Injury: A Systematic Review and Meta-
939 analysis. *JAMA Neurol.* 2019;76(1):81-94.
- 940 17. Wardlaw JM, Smith EE, Biessels GJ, Cordonnier C, Fazekas F, Frayne R, et al.
941 Neuroimaging standards for research into small vessel disease and its contribution to ageing and
942 neurodegeneration. *Lancet Neurol.* 2013;12(8):822-38.
- 943 18. DeBette S, Markus HS. The clinical importance of white matter hyperintensities on brain
944 magnetic resonance imaging: systematic review and meta-analysis. *BMJ.* 2010;341:c3666.
- 945 19. King KS, Chen KX, Hulsey KM, McColl RW, Weiner MF, Nakonezny PA, et al. White
946 matter hyperintensities: use of aortic arch pulse wave velocity to predict volume independent of other
947 cardiovascular risk factors. *Radiology.* 2013;267(3):709-17.
- 948 20. Mitchell GF, van Buchem MA, Sigurdsson S, Gotal JD, Jonsdottir MK, Kjartansson O, et al.
949 Arterial stiffness, pressure and flow pulsatility and brain structure and function: the Age,
950 Gene/Environment Susceptibility--Reykjavik study. *Brain.* 2011;134(Pt 11):3398-407.
- 951 21. Henskens LH, Kroon AA, van Oostenbrugge RJ, Gronenschild EH, Fuss-Lejeune MM,
952 Hofman PA, et al. Increased aortic pulse wave velocity is associated with silent cerebral small-vessel
953 disease in hypertensive patients. *Hypertension.* 2008;52(6):1120-6.
- 954 22. Cocciolone AJ, Hawes JZ, Staiculescu MC, Johnson EO, Murshed M, Wagenseil JE. Elastin,
955 arterial mechanics, and cardiovascular disease. *American journal of physiology Heart and circulatory*
956 *physiology.* 2018;315(2):H189-H205.
- 957 23. Duca L, Blaise S, Romier B, Laffargue M, Gayral S, El Btaouri H, et al. Matrix ageing and
958 vascular impacts: focus on elastin fragmentation. *Cardiovascular research.* 2016;110(3):298-308.
- 959 24. Ferrucci L, Fabbri E. Inflammageing: chronic inflammation in ageing, cardiovascular disease,
960 and frailty. *Nature reviews Cardiology.* 2018;15(9):505-22.
- 961 25. Bai W SH, Qin C, Tarroni G, Oktay O, Matthews PM, Rueckert D. Recurrent Neural
962 Networks for Aortic Image Sequence Segmentation with Sparse Annotations. In: Frangi A, Schnabel
963 J, Davatzikos C, Alberola-López C, Fichtinger G (eds) *Medical Image Computing and Computer*
964 *Assisted Intervention – MICCAI 2018.* 2018;MICCAI 2018. *Lecture Notes in Computer Science*, vol
965 11073. Springer, Cham. .
- 966 26. Littlejohns TJ, Holliday J, Gibson LM, Garratt S, Oesingmann N, Alfaro-Almagro F, et al.
967 The UK Biobank imaging enhancement of 100,000 participants: rationale, data collection,
968 management and future directions. *Nat Commun.* 2020;11(1):2624.
- 969 27. Bai W, Suzuki H, Huang J, Francis C, Wang S, Tarroni G, et al. A population-based
970 phenome-wide association study of cardiac and aortic structure and function. *Nature medicine.*
971 2020;26(10):1654-62.
- 972 28. Turley P, Walters RK, Maghzian O, Okbay A, Lee JJ, Fontana MA, et al. Multi-trait analysis
973 of genome-wide association summary statistics using MTAG. *Nature genetics.* 2018;50(2):229-37.
- 974 29. Consortium G. GTEx v8 2021: <https://gtexportal.org/home/>.
- 975 30. Pirruccello J. Deep learning enables genetic analysis of the human thoracic aorta. *BioRxiv.*
976 2020;doi <https://doi.org/10.1101/2020.05.12.091934>.
- 977 31. Tcheandjieu C. High heritability of ascending aortic diameter and multi-ethnic prediction of
978 thoracic aortic disease. *MedRxiv.* 2021;doi: <https://doi.org/10.1101/2020.05.29.20102335>.
- 979 32. Watanabe K, Taskesen E, van Bochoven A, Posthuma D. Functional mapping and annotation
980 of genetic associations with FUMA. *Nature communications.* 2017;8(1):1826.
- 981 33. de Leeuw CA, Mooij JM, Heskes T, Posthuma D. MAGMA: generalized gene-set analysis of
982 GWAS data. *PLoS computational biology.* 2015;11(4):e1004219.
- 983 34. Zhang W, Zhang S, Yan P, Ren J, Song M, Li J, et al. A single-cell transcriptomic landscape
984 of primate arterial aging. *Nature communications.* 2020;11(1):2202.
- 985 35. Evangelou E, Warren HR, Mosen-Ansorena D, Mifsud B, Pazoki R, Gao H, et al. Genetic
986 analysis of over 1 million people identifies 535 new loci associated with blood pressure traits. *Nature*
987 *genetics.* 2018;50(10):1412-25.

- 988 36. Tzourio C, Cohen A, Lamisse N, Biousse V, Bousser MG. Aortic root dilatation in patients
989 with spontaneous cervical artery dissection. *Circulation*. 1997;95(10):2351-3.
- 990 37. Sargurupremraj M, Suzuki H, Jian X, Sarnowski C, Evans TE, Bis JC, et al. Cerebral small
991 vessel disease genomics and its implications across the lifespan. *Nature communications*.
992 2020;11(1):6285.
- 993 38. Kozel BA, Barak B, Kim CA, Mervis CB, Osborne LR, Porter M, et al. Williams syndrome.
994 *Nat Rev Dis Primers*. 2021;7(1):42.
- 995 39. Elbitar S, Renard M, Arnaud P, Hanna N, Jacob MP, Guo DC, et al. Pathogenic variants in
996 THSD4, encoding the ADAMTS-like 6 protein, predispose to inherited thoracic aortic aneurysm.
997 *Genetics in medicine : official journal of the American College of Medical Genetics*. 2021;23(1):111-
998 22.
- 999 40. Van Maldergem L, Loeys B. FBLN5-Related Cutis Laxa. In: Pagon RA, Adam MP, Ardinger
1000 HH, Bird TD, Dolan CR, Fong CT, et al., editors. *GeneReviews(R)*. Seattle (WA)1993.
- 1001 41. Loeys B, Van Maldergem L, Mortier G, Coucke P, Gerniers S, Naeyaert JM, et al.
1002 Homozygosity for a missense mutation in fibulin-5 (FBLN5) results in a severe form of cutis laxa.
1003 *Human molecular genetics*. 2002;11(18):2113-8.
- 1004 42. Li N, Subrahmanyam L, Smith E, Yu X, Zaidi S, Choi M, et al. Mutations in the Histone
1005 Modifier PRDM6 Are Associated with Isolated Nonsyndromic Patent Ductus Arteriosus. *American
1006 journal of human genetics*. 2016;99(4):1000.
- 1007 43. Hiraki Y, Miyatake S, Hayashidani M, Nishimura Y, Matsuura H, Kamada M, et al. Aortic
1008 aneurysm and craniosynostosis in a family with Cantu syndrome. *American journal of medical
1009 genetics Part A*. 2014;164A(1):231-6.
- 1010 44. Dietz HC, Cutting GR, Pyeritz RE, Maslen CL, Sakai LY, Corson GM, et al. Marfan
1011 syndrome caused by a recurrent de novo missense mutation in the fibrillin gene. *Nature*.
1012 1991;352(6333):337-9.
- 1013 45. Walsh R, Rutland C, Thomas R, Loughna S. Cardiomyopathy: a systematic review of disease-
1014 causing mutations in myosin heavy chain 7 and their phenotypic manifestations. *Cardiology*.
1015 2010;115(1):49-60.
- 1016 46. Kirk EP, Sunde M, Costa MW, Rankin SA, Wolstein O, Castro ML, et al. Mutations in
1017 cardiac T-box factor gene TBX20 are associated with diverse cardiac pathologies, including defects
1018 of septation and valvulogenesis and cardiomyopathy. *American journal of human genetics*.
1019 2007;81(2):280-91.
- 1020 47. Rooryck C, Diaz-Font A, Osborn DP, Chabchoub E, Hernandez-Hernandez V, Shamseldin H,
1021 et al. Mutations in lectin complement pathway genes COLEC11 and MASP1 cause 3MC syndrome.
1022 *Nature genetics*. 2011;43(3):197-203.
- 1023 48. Guo DC, Regalado ES, Gong L, Duan X, Santos-Cortez RL, Arnaud P, et al. LOX Mutations
1024 Predispose to Thoracic Aortic Aneurysms and Dissections. *Circulation research*. 2016;118(6):928-34.
- 1025 49. Guo DC, Grove ML, Prakash SK, Eriksson P, Hostetler EM, LeMaire SA, et al. Genetic
1026 Variants in LRP1 and ULK4 Are Associated with Acute Aortic Dissections. *American journal of
1027 human genetics*. 2016;99(3):762-9.
- 1028 50. Pyeritz RE. Heritable thoracic aortic disorders. *Current opinion in cardiology*. 2014;29(1):97-
1029 102.
- 1030 51. MacCarrick G, Black JH, 3rd, Bowdin S, El-Hamamsy I, Frischmeyer-Guerrero PA,
1031 Guerrero AL, et al. Loeys-Dietz syndrome: a primer for diagnosis and management. *Genetics in
1032 medicine : official journal of the American College of Medical Genetics*. 2014;16(8):576-87.
- 1033 52. Duan C, Xu Q. Roles of insulin-like growth factor (IGF) binding proteins in regulating IGF
1034 actions. *Gen Comp Endocrinol*. 2005;142(1-2):44-52.
- 1035 53. von der Thusen JH, Borensztajn KS, Moimas S, van Heiningen S, Teeling P, van Berkel TJ,
1036 et al. IGF-1 has plaque-stabilizing effects in atherosclerosis by altering vascular smooth muscle cell
1037 phenotype. *The American journal of pathology*. 2011;178(2):924-34.

- 1038 54. Lei Y, Yi Y, Liu Y, Liu X, Keller ET, Qian CN, et al. Metformin targets multiple signaling
1039 pathways in cancer. *Chin J Cancer*. 2017;36(1):17.
- 1040 55. Fujimura N, Xiong J, Kettler EB, Xuan H, Glover KJ, Mell MW, et al. Metformin treatment
1041 status and abdominal aortic aneurysm disease progression. *Journal of vascular surgery*.
1042 2016;64(1):46-54 e8.
- 1043 56. Lareyre F, Raffort J. Metformin to Limit Abdominal Aortic Aneurysm Expansion: Time for
1044 Clinical Trials. *European journal of vascular and endovascular surgery : the official journal of the*
1045 *European Society for Vascular Surgery*. 2021;61(6):1030.
- 1046 57. Lopes-Ramos CM, Chen CY, Kuijjer ML, Paulson JN, Sonawane AR, Fagny M, et al. Sex
1047 Differences in Gene Expression and Regulatory Networks across 29 Human Tissues. *Cell Rep*.
1048 2020;31(12):107795.
- 1049 58. Nethononda RM, Lewandowski AJ, Stewart R, Kylinterias I, Whitworth P, Francis J, et al.
1050 Gender specific patterns of age-related decline in aortic stiffness: a cardiovascular magnetic
1051 resonance study including normal ranges. *Journal of cardiovascular magnetic resonance : official*
1052 *journal of the Society for Cardiovascular Magnetic Resonance*. 2015;17:20.
- 1053 59. Tadros R, Francis C, Xu X, Vermeer AMC, Harper AR, Huurman R, et al. Shared genetic
1054 pathways contribute to risk of hypertrophic and dilated cardiomyopathies with opposite directions of
1055 effect. *Nature genetics*. 2021;53(2):128-34.
- 1056 60. Davis EC. Elastic lamina growth in the developing mouse aorta. *The journal of*
1057 *histochemistry and cytochemistry : official journal of the Histochemistry Society*. 1995;43(11):1115-
1058 23.
- 1059 61. Wahart A, Hocine T, Albrecht C, Henry A, Sarazin T, Martiny L, et al. Role of elastin
1060 peptides and elastin receptor complex in metabolic and cardiovascular diseases. *The FEBS journal*.
1061 2019.
- 1062 62. Urban Z, Riazi S, Seidl TL, Katahira J, Smoot LB, Chitayat D, et al. Connection between
1063 elastin haploinsufficiency and increased cell proliferation in patients with supravalvular aortic
1064 stenosis and Williams-Beuren syndrome. *American journal of human genetics*. 2002;71(1):30-44.
- 1065 63. Papke CL, Yanagisawa H. Fibulin-4 and fibulin-5 in elastogenesis and beyond: Insights from
1066 mouse and human studies. *Matrix Biol*. 2014;37:142-9.
- 1067 64. Nead KT, Li A, Wehner MR, Neupane B, Gustafsson S, Butterworth A, et al. Contribution of
1068 common non-synonymous variants in PCSK1 to body mass index variation and risk of obesity: a
1069 systematic review and meta-analysis with evidence from up to 331 175 individuals. *Human*
1070 *molecular genetics*. 2015;24(12):3582-94.
- 1071 65. Consortium CAD, Deloukas P, Kanoni S, Willenborg C, Farrall M, Assimes TL, et al. Large-
1072 scale association analysis identifies new risk loci for coronary artery disease. *Nature genetics*.
1073 2013;45(1):25-33.
- 1074 66. Baxter BT, Davis VA, Minion DJ, Wang YP, Lynch TG, McManus BM. Abdominal aortic
1075 aneurysms are associated with altered matrix proteins of the nonaneurysmal aortic segments. *Journal*
1076 *of vascular surgery*. 1994;19(5):797-802; discussion 3.
- 1077 67. International Consortium for Blood Pressure Genome-Wide Association S, Ehret GB, Munroe
1078 PB, Rice KM, Bochud M, Johnson AD, et al. Genetic variants in novel pathways influence blood
1079 pressure and cardiovascular disease risk. *Nature*. 2011;478(7367):103-9.
- 1080 68. O'Rourke MF, Safar ME. Relationship between aortic stiffening and microvascular disease in
1081 brain and kidney: cause and logic of therapy. *Hypertension*. 2005;46(1):200-4.
- 1082 69. Lacolley P, Regnault V, Segers P, Laurent S. Vascular Smooth Muscle Cells and Arterial
1083 Stiffening: Relevance in Development, Aging, and Disease. *Physiol Rev*. 2017;97(4):1555-617.
- 1084 70. Jefferson AL, Cambrono FE, Liu D, Moore EE, Neal JE, Terry JG, et al. Higher Aortic
1085 Stiffness Is Related to Lower Cerebral Blood Flow and Preserved Cerebrovascular Reactivity in
1086 Older Adults. *Circulation*. 2018;138(18):1951-62.
- 1087 71. Coronary Artery Disease Genetics C. A genome-wide association study in Europeans and
1088 South Asians identifies five new loci for coronary artery disease. *Nature genetics*. 2011;43(4):339-44.

- 1089 72. Beaudoin M, Gupta RM, Won HH, Lo KS, Do R, Henderson CA, et al. Myocardial
1090 Infarction-Associated SNP at 6p24 Interferes With MEF2 Binding and Associates With PHACTR1
1091 Expression Levels in Human Coronary Arteries. *Arteriosclerosis, thrombosis, and vascular biology*.
1092 2015;35(6):1472-9.
- 1093 73. Anttila V, Winsvold BS, Gormley P, Kurth T, Bettella F, McMahon G, et al. Genome-wide
1094 meta-analysis identifies new susceptibility loci for migraine. *Nature genetics*. 2013;45(8):912-7.
- 1095 74. Kiando SR, Tucker NR, Castro-Vega LJ, Katz A, D'Escamard V, Treard C, et al. PHACTR1
1096 Is a Genetic Susceptibility Locus for Fibromuscular Dysplasia Supporting Its Complex Genetic
1097 Pattern of Inheritance. *PLoS genetics*. 2016;12(10):e1006367.
- 1098 75. Debette S, Kamatani Y, Metso TM, Kloss M, Chauhan G, Engelter ST, et al. Common
1099 variation in PHACTR1 is associated with susceptibility to cervical artery dissection. *Nature genetics*.
1100 2015;47(1):78-83.
- 1101 76. Petersen SE, Matthews PM, Francis JM, Robson MD, Zemrak F, Boubertakh R, et al. UK
1102 Biobank's cardiovascular magnetic resonance protocol. *Journal of cardiovascular magnetic resonance*
1103 : official journal of the Society for Cardiovascular Magnetic Resonance. 2016;18:8.
- 1104 77. Loh PR, Tucker G, Bulik-Sullivan BK, Vilhjalmsson BJ, Finucane HK, Salem RM, et al.
1105 Efficient Bayesian mixed-model analysis increases association power in large cohorts. *Nature*
1106 *genetics*. 2015;47(3):284-90.
- 1107 78. Altman DG, Bland JM. Interaction revisited: the difference between two estimates. *BMJ*.
1108 2003;326(7382):219.
- 1109 79. Quinlan AR, Hall IM. BEDTools: a flexible suite of utilities for comparing genomic features.
1110 *Bioinformatics*. 2010;26(6):841-2.
- 1111 80. Pers TH, Karjalainen JM, Chan Y, Westra HJ, Wood AR, Yang J, et al. Biological
1112 interpretation of genome-wide association studies using predicted gene functions. *Nature*
1113 *communications*. 2015;6:5890.
- 1114 81. Purcell S, Neale B, Todd-Brown K, Thomas L, Ferreira MA, Bender D, et al. PLINK: a tool
1115 set for whole-genome association and population-based linkage analyses. *American journal of human*
1116 *genetics*. 2007;81(3):559-75.
- 1117 82. Bulik-Sullivan BK, Loh PR, Finucane HK, Ripke S, Yang J, Schizophrenia Working Group
1118 of the Psychiatric Genomics C, et al. LD Score regression distinguishes confounding from
1119 polygenicity in genome-wide association studies. *Nature genetics*. 2015;47(3):291-5.
- 1120 83. McCarthy DJ, Campbell KR, Lun AT, Wills QF. Scater: pre-processing, quality control,
1121 normalization and visualization of single-cell RNA-seq data in R. *Bioinformatics*. 2017;33(8):1179-
1122 86.
- 1123 84. Lun AT, McCarthy DJ, Marioni JC. A step-by-step workflow for low-level analysis of single-
1124 cell RNA-seq data with Bioconductor. *F1000Res*. 2016;5:2122.
- 1125 85. Yu G, Wang LG, Han Y, He QY. clusterProfiler: an R package for comparing biological
1126 themes among gene clusters. *Omics : a journal of integrative biology*. 2012;16(5):284-7.
- 1127 86. Burgess S, Foley CN, Allara E, Staley JR, Howson JMM. A robust and efficient method for
1128 Mendelian randomization with hundreds of genetic variants. *Nature communications*.
1129 2020;11(1):376.
- 1130 87. Burgess S, Small DS, Thompson SG. A review of instrumental variable estimators for
1131 Mendelian randomization. *Statistical methods in medical research*. 2017;26(5):2333-55.
- 1132 88. Bowden J, Davey Smith G, Haycock PC, Burgess S. Consistent Estimation in Mendelian
1133 Randomization with Some Invalid Instruments Using a Weighted Median Estimator. *Genetic*
1134 *epidemiology*. 2016;40(4):304-14.
- 1135 89. Burgess S, Thompson SG. Interpreting findings from Mendelian randomization using the
1136 MR-Egger method. *European journal of epidemiology*. 2017;32(5):377-89.
- 1137 90. Verbanck M, Chen CY, Neale B, Do R. Detection of widespread horizontal pleiotropy in
1138 causal relationships inferred from Mendelian randomization between complex traits and diseases.
1139 *Nature genetics*. 2018;50(5):693-8.

- 1140 91. Bowden J, Spiller W, Del Greco MF, Sheehan N, Thompson J, Minelli C, et al. Improving the
1141 visualization, interpretation and analysis of two-sample summary data Mendelian randomization via
1142 the Radial plot and Radial regression. *Int J Epidemiol*. 2018;47(4):1264-78.
- 1143 92. Bowden J, Davey Smith G, Burgess S. Mendelian randomization with invalid instruments:
1144 effect estimation and bias detection through Egger regression. *Int J Epidemiol*. 2015;44(2):512-25.
- 1145 93. Sanderson E, Davey Smith G, Windmeijer F, Bowden J. An examination of multivariable
1146 Mendelian randomization in the single-sample and two-sample summary data settings. *Int J*
1147 *Epidemiol*. 2019;48(3):713-27.
- 1148 94. Wu P, Gifford A, Meng X, Li X, Campbell H, Varley T, et al. Mapping ICD-10 and ICD-10-
1149 CM Codes to Phecodes: Workflow Development and Initial Evaluation. *JMIR Med Inform*.
1150 2019;7(4):e14325.
- 1151 95. Bulik-Sullivan B, Finucane HK, Anttila V, Gusev A, Day FR, Loh PR, et al. An atlas of
1152 genetic correlations across human diseases and traits. *Nature genetics*. 2015;47(11):1236-41.
- 1153 96. Shi H, Mancuso N, Spendlove S, Pasaniuc B. Local Genetic Correlation Gives Insights into
1154 the Shared Genetic Architecture of Complex Traits. *American journal of human genetics*.
1155 2017;101(5):737-51.
- 1156 97. Pickrell JK, Berisa T, Liu JZ, Segurel L, Tung JY, Hinds DA. Detection and interpretation of
1157 shared genetic influences on 42 human traits. *Nature genetics*. 2016;48(7):709-17.
- 1158 98. Pickrell JK. Joint analysis of functional genomic data and genome-wide association studies of
1159 18 human traits. *American journal of human genetics*. 2014;94(4):559-73.
- 1160 99. Berisa T, Pickrell JK. Approximately independent linkage disequilibrium blocks in human
1161 populations. *Bioinformatics*. 2016;32(2):283-5.
1162